

Mn AND S³⁺ PARTITIONING IN SULPHIDES-
A COMPARISON OF TWO GEOTHERMOMETERS

By

ROBERT L. WRIGHT

A Thesis

Submitted to the Faculty of Arts and Sciences
in Partial Fulfillment of the Requirements
for the Degree
Bachelor of Science

McMaster University

May 1971

ABSTRACT

Sulphide samples from high and low temperature environments were used to compare two recently calibrated geothermometers :

- 1) The distribution of MnS between coexisting galena and sphalerite.
- 2) The fractionation of sulphur isotopes between coexisting sulphide minerals.

The manganese analyses were done by two neutron activation procedures. For the high temperature environment, the MnS temperatures are significantly lower than the sulphur isotope temperatures; these results are reasonable if one accepts an hypothesis of limited subsolidus re-equilibration of sulphur isotopes, but extensive redistribution of manganese. The sulphur isotope results for the low temperature deposit are also acceptable, but the manganese temperatures are too high, due to analytical errors (resulting from low concentrations, and possible contamination), or to lack of equilibrium in the samples themselves.

The extension of the sulphur isotope geothermometer to low temperatures (100-200°C) appears to be justified, whereas the results for the MnS geothermometer are inconclusive.

ACKNOWLEDGEMENTS

The author wishes to express his gratitude to Dr. J.H. Crocket and Dr. H.P. Schwarcz, who supervised this project. Dr. Crocket provided the equipment and knowledge of experimental techniques which were invaluable in the neutron activation work. Dr. Schwarcz provided the equipment and knowledge which made the sulphur isotope work possible.

Mrs. Jill Gleed assisted in the preparation of SO₂ samples; Mr. Len Falkiner prepared the X-ray diffraction traces; faculty and fellow students provided helpful discussions. Their assistance is gratefully acknowledged.

I particularly wish to thank Mr. David Wright, who gave up many hours of his time to assist with the mineral separations, calculations, and typing.

TABLE OF CONTENTS

Abstract	ii
Acknowledgements	iii
Introduction	1
A) Purpose	1
B) Location and Description of Samples	1
a) Keymet Mine	1
b) Dundas	3
c) Sample Numbers	3
Procedure	6
A) Sample Preparation	6
B) MnS Determination	6
a) Standards	6
b) Non-destructive Procedure	8
c) Wet-chemical Procedure	8
d) Calculations	10
C) Sulphur Isotopes	10
a) Preparation of SO ₂	10
b) Measurement of δS^{34} values	11
c) Calculations	11
Experimental Results	12
A) Sample Purity	12
B) Manganese Analyses	12
C) Sulphur Isotopes	15
Discussion	17
A) Precision and Accuracy in Mn Analyses	17
B) The MnS Geothermometer	18

C) Sulphur Isotopes	23
D) Comparison of Temperature Results	25
a) Keymet	25
b) Dundas	29
E) Origin of the Deposits	29
a) Keymet	29
b) Dundas	30
Conclusions	32
Suggestions for Further Study	33
Bibliography	34
Appendix 1	38
Appendix 2	42
Appendix 3	45

LIST OF TABLES

1	Purity of samples as determined by X-ray diffraction	13
2	Manganese concentrations in coexisting sulphides	14
3	δS^{34} values of sphalerite	15
4	$\Delta_{ab}(\text{‰})$ values of coexisting sulphides	16
5	Temperature results from the MnS geothermometer	22
6	Temperature results from sulphur isotopes	24
7	Comparison of temperatures from the two geothermometers	24
8	Nuclear reactions involved in manganese determination	39
9	Correction of Mn analyses for $Fe^{56}(n,p)Mn^{56}$ contribution	40

LIST OF FIGURES

1	General location of samples	2
2	Textural features of samples	4
3	Sample preparation	7
4	Effect of contamination of galena by sphalerite	19
5	MnS geothermometer	21
6	Sulphur isotope fractionation (Grootenboer & Schwarcz, 1969)	26
7	Sulphur isotope fractionation (Kajiwara & Krouse, 1970)	27
8	Graphical illustration of relationship between counting interval and time of accumulation of half the total counts	44
9	Effect of smoothing on the shape of the Gaussian function	52

INTRODUCTION

A) PURPOSE

This study was undertaken to compare the temperatures obtained for sulphide samples, using two experimentally calibrated geothermometers - the distribution of manganese between coexisting galena and sphalerite (Bethke and Barton, 1971) and the fractionation of sulphur isotopes between the same minerals (Grootenboer and Schwarcz, 1965, Rye and Czamanske, 1969, and Kajiwara and Krouse, 1970). Two samples of ore from the Keymet Mine, near Bathurst, New Brunswick, were studied. An additional objective was to determine whether these geothermometers, which were calibrated at fairly high temperatures, could be extended to low temperatures. For this purpose, samples of Mississippi Valley type sulphide veins from Dundas, Ontario, were included (see Figure 1 for general location).

B) LOCATION AND DESCRIPTION OF SAMPLES

a) Keymet Mine

The geology of the ore deposits of northern New Brunswick has been summarized by Davies (1966). Greiner and Potter (1966) discuss the regional stratigraphy, and present a map of the area. The geology of the Keymet Mine itself is discussed by Roy (1961). The deposit consists of lenses and veins of sulphides in a fault which cuts shale, conglomerate, and argillite of Middle to Upper Silurian age. The mine is separated from a number of massive sulphide deposits to the south by a major discontinuity, the Rocky Brook - Millstream fault.

The ores consist of pyrite, arsenopyrite, sphalerite, galena, chalcopyrite, pyrrhotite, tetrahedrite, and calcite, which crystallized

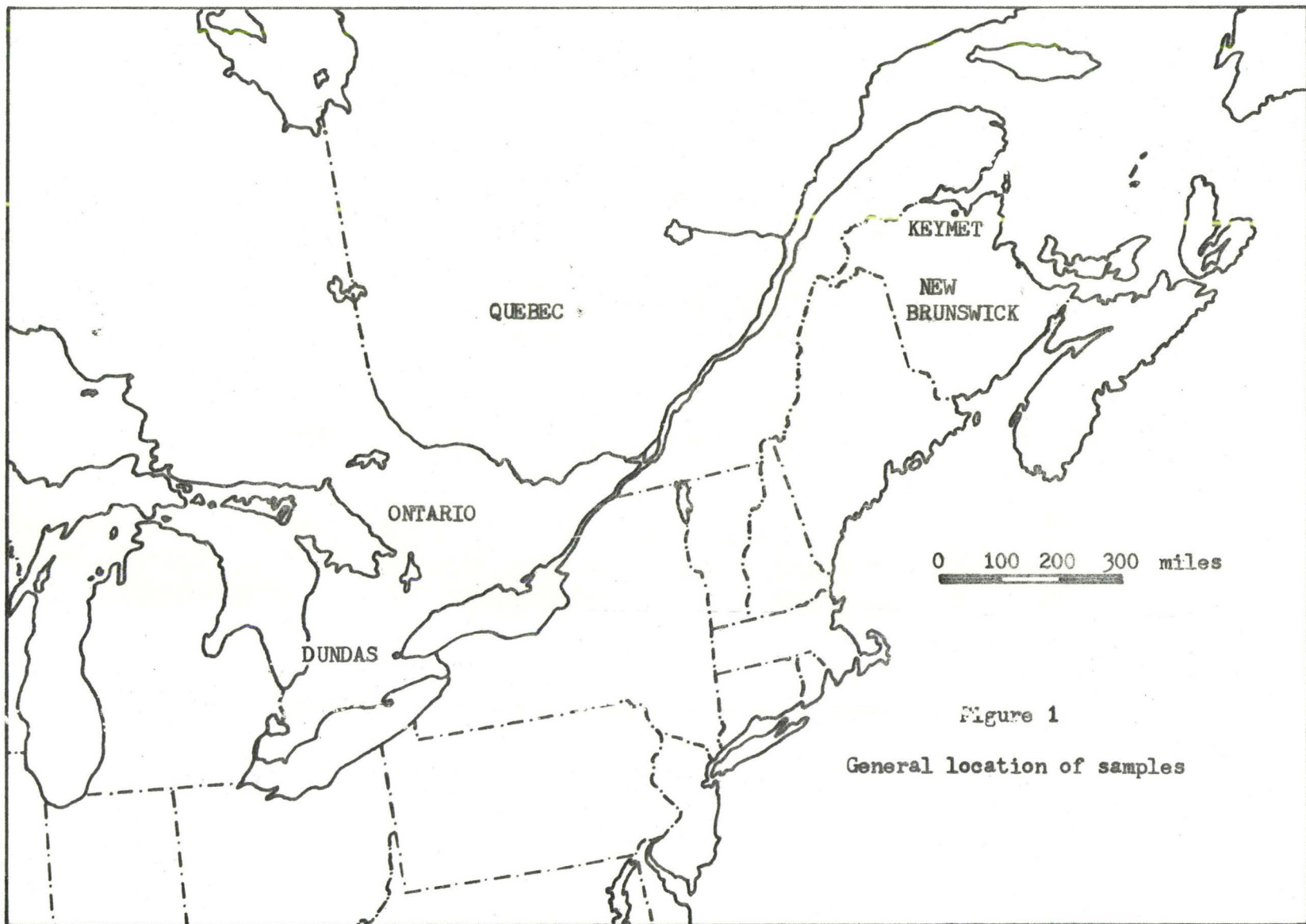


Figure 1
General location of samples

approximately in that order. The relation of galena and arsenopyrite to the paragenesis is disputed (see Roy, 1961).

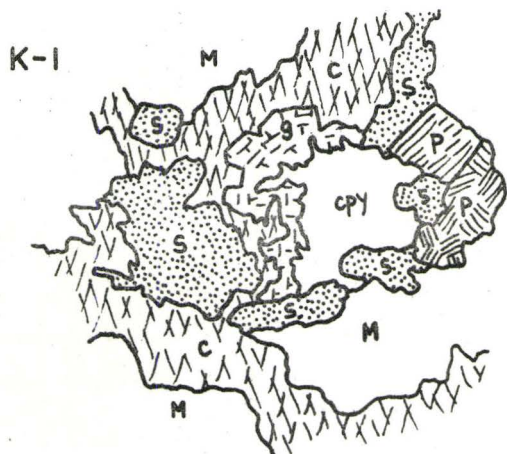
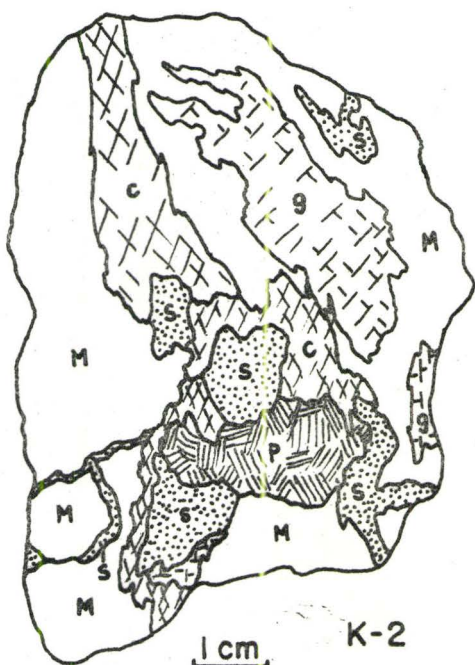
Both ore samples were obtained from the dumps at Keymet, since the mine had closed down, at a depth of 1200 feet. Sample K-1 consists of subhedral to euhedral pyrite, sphalerite, and galena, with chalcopyrite replacing (?) and veining the earlier sulphides. The sample is veined by calcite. Sample K-2 consists of lenses and stringers of the same sulphides (excluding chalcopyrite) in a pale green, fine-grained matrix. The paragenetic sequence appears to be the same as in K-1. Figure 2 shows the textural relationships of these samples.

b) Dundas

The geology of the area is discussed in reports by Caley (1961) and Beards (1967). The samples were collected in the quarry of Canada Crushed and Cut Stone Ltd., which is in massive limestones and dolomites of Silurian age. The sulphides occur in veins cutting the dolomite. Massive pyrite and/or marcasite was the first phase to form, prior to sphalerite and galena, and then calcite. Some late pyrite is also present as crystals lining cavities in massive sphalerite. The three samples (only two were analysed for manganese) are quite similar, consisting of massive sphalerite, with cavities lined by pyrite or sphalerite and galena crystals. This massive sphalerite is covered by a layer of galena and sphalerite crystals, and by calcite. The galena and sphalerite concentrates were from this latter mode of occurrence (see Figure 2 for textural features).

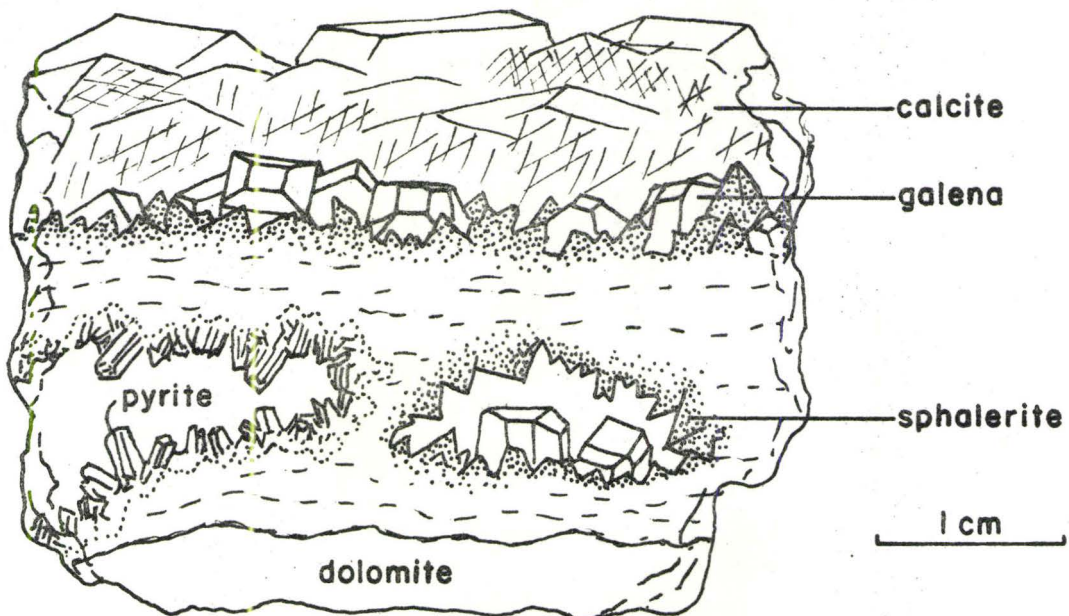
c) Sample Numbers

All concentrates were assigned a three-part name to facilitate identification. The first letter, a K or D, indicates Keymet or Dundas



- g - galena
- c - calcite
- p - pyrite
- s - sphalerite
- m - matrix
- cpy - chalcopyrite

KEYMET



DUNDAS

Figure 2 Textural features of samples.

respectively; the second letter(s), S, G, P, C, or Cpy indicates sphalerite, galena, pyrite, calcite, or chalcopyrite, respectively. This is followed by the sample number; hence, KC-2 is the calcite concentrate from Keymet sample number 2.

PROCEDURE

A) SAMPLE PREPARATION

Mineral concentrates were produced by hand picking, magnetic separation, and acid leaching, as outlined in Figure 3. All samples were X-rayed to confirm the identification of the mineral of interest and to check for impurities.

B) MnS DETERMINATION

Manganese was determined by neutron activation analysis, using either a non-destructive or a wet-chemical, carrier based procedure, depending on concentration.

a) Standards

For samples with more than 100 ppm Mn, as determined by preliminary experiments, a National Bureau of Standards steel, 19G, with reported analysis $0.554 \pm 0.005\%$ Mn, was used. This was weighed into quartz ampoules, which were sealed with an oxygen-gas flame.

For samples with 1 to 100 ppm Mn, a liquid standard was prepared by weighing out 10 milligrams of Johnson Matthey and Mallory Specpure MnO_2 , and dissolving in 100 mg. of 6M HCl. This liquid (approximately 50 mg.) was weighed into quartz ampoules. Quartz powder, prepared from the same tubing as the ampoules, was added to adsorb the manganese. The standards were evaporated to dryness at $80^\circ C$ for 12 hours then sealed as before.

For samples with less than 1 ppm Mn, the above standard solution was diluted 100-fold with 6M HCl, then weighed into ampoules, evaporated onto quartz powder, then sealed.

Standard blanks, to monitor Mn in the HCl used in standard

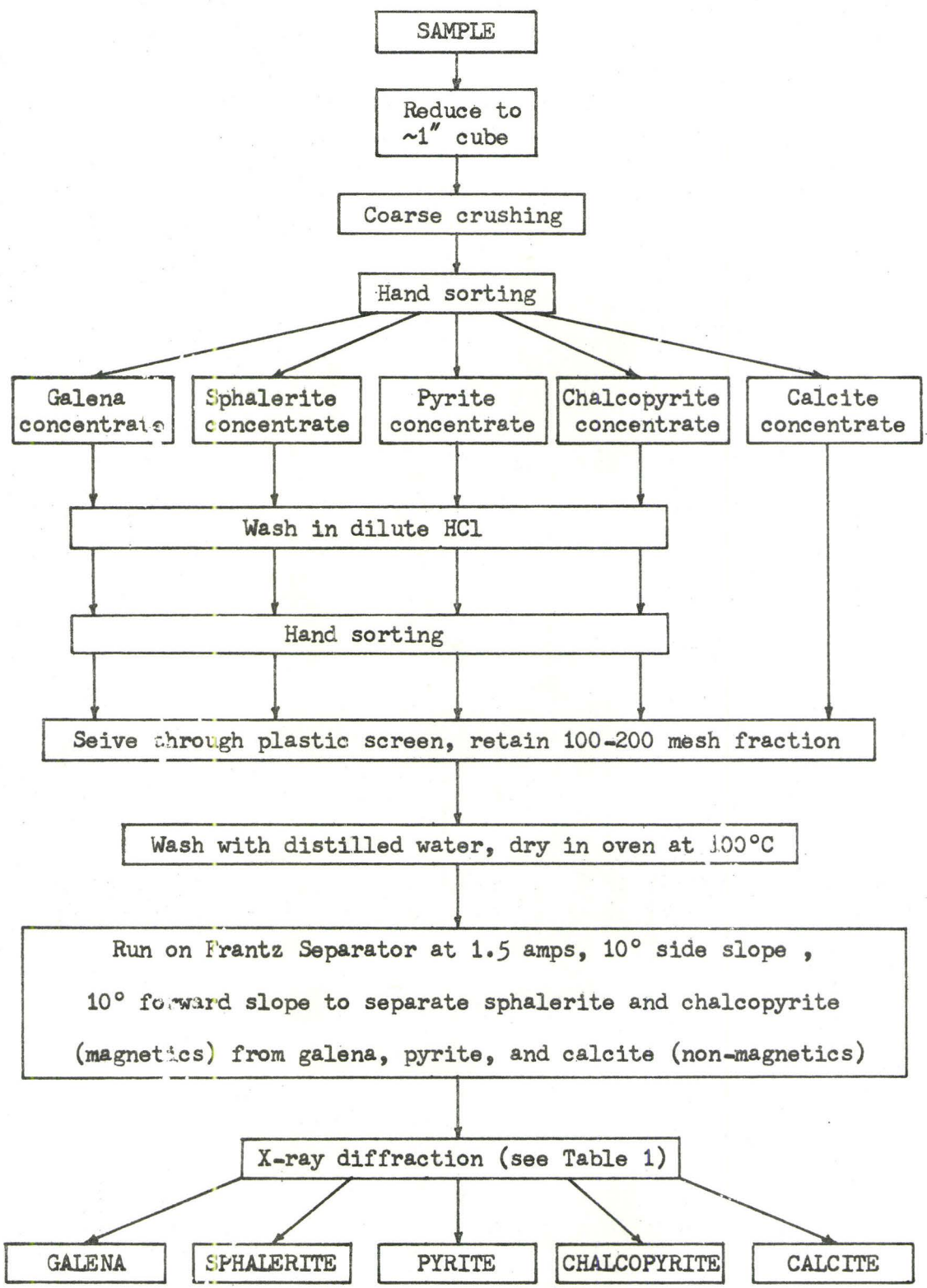


Figure 3 - Sample Preparation

solutions, were prepared by treating 6M HCl in the same way as the standard solutions.

b) Non-destructive Procedure

Samples were weighed into quartz ampoules and sealed. Sample blanks were prepared by sealing empty ampoules. Standards, samples, and blanks were sealed in an aluminum can and irradiated in a high flux position (approximately 1×10^{13} neutrons/cm²/sec) for 2 minutes in the McMaster Research Reactor.

After cooling, the ampoules were rinsed in acetone and placed unopened, in glass screw-top vials, which were then sealed with masking tape. Samples and standards were counted with a 25cc Li-drifted germanium diode coupled to a 1600 channel gamma radiation analyser and memory. Counting times varied from 5 to 25 minutes, depending on the counting rate. The appropriate blank was counted in the subtract mode for the same period of time, so that the background and blank contributions (eg Mn in the HCl) were automatically eliminated.

c) Wet-chemical Procedure

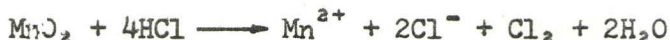
The manganese activity in the Dundas galena samples was too low to determine by non-destructive counting due to interfering radionuclides, notably arsenic, so that a chemical separation, after irradiation, was necessary.

1) Samples, standards, and standard blank were irradiated for 10 minutes and cooled for 1 hour.

2) Ampoules were opened and rinsed into 250 ml. beakers containing 50 µg. As₂O₃ and 10 mg. Mn (a Mn carrier was previously

prepared by dissolving 100 mg. Mn, as MnO_2 , in 100 ml. 6M HCl. 10 ml. aliquots were transferred to each beaker).

3) The samples were dissolved in 20 ml. hot 12M HCl and the solution diluted to 60 ml. Although the manganese in sphalerite and galena is Mn^{2+} , while MnO_2 contains Mn^{4+} , homogenization occurs due to the reaction (Cotton and Wilkinson, 1962):



4) Approximately 1 gram of thioacetamide was added, resulting in a yellow precipitate of As_2S_3 .

5) The precipitate was digested at 100°C for 15 minutes, to ensure complete precipitation and removal of excess H_2S .

6) The solution (containing the Mn) was filtered, transferred to a 50 ml. volumetric flask, and made up to volume with 6M HCl.

The samples, standards, and blank were counted, in the flasks, with a thallium-doped 3" x 3" well-type NaI detector coupled to the 1600 channel memory. Counting time was 3 minutes; blank and background were automatically subtracted, as before.

The yield of manganese in the chemical separation was determined, after counting, by the following procedure (after Hillebrand et al, 1953, and Kolthoff and Sandell, 1952):

1) Samples were transferred quantitatively to a 250 ml. beaker
 2) Chloride was removed by adding 15 ml. HNO_3 and 10 ml. H_2SO_4 then evaporating to fumes of SO_3 .

3) After diluting to 80 ml., 5 ml. H_3PO_4 and 0.5 grams KIO_4 were added, and the solution boiled for 1 minute, kept hot 5 minutes, then cooled. A precipitate of $PbSO_4$ (identified by X-ray diffraction) formed at this time in the galena sample solutions.

4) The resulting permanganate solution was transferred quantitatively to a 100 ml. volumetric flask and made up to volume. A 10 ml. aliquot of this solution was then diluted to 100 ml., to produce a solution with about 1 mg. Mn per 100 ml.

5) Permanganate was determined spectrophotometrically at 525 m μ , using a Rausch and Lomb Spectronic 20.

d) Calculations

The area under the 0.845 Mev manganese peak was determined for each sample and standard (see Appendix 3). The standard peak areas were plotted on a semi-logarithmic graph, and corrected for decay to the appropriate sample counting time. The counting time was taken as the time at which half the total counts for that sample had accumulated. This is, in general, less than half the counting interval, because the sample is decaying during counting (see Appendix 2). In the case of Mn⁵⁶, however, this time was within a few seconds of the mid-point in the counting interval; for example, if a sample was counted for 10 minutes, starting at 1:00 o'clock, the counting time would be taken as 1:05.

C) SULPHUR ISOTOPES

a) Preparation of SO₂

The sulphur was extracted from the sulphide samples by burning at 1400°C in a stream of purified oxygen to produce SO₂ which was sealed in a pyrex breakseal, after removal of excess oxygen, water, and CO₂. Details of the apparatus and procedure are described by Thode et al (1961).

b) Measurement of δS^{34} Values

The SO_2 was analysed on a 6 inch, 90° double-collecting mass spectrometer described by Wanless and Thode (1953). The sphalerite samples were compared with a working standard, a pyrite sample from Park City, Utah, which in turn was compared with troilite sulphur from the Canon Diablo meteorite. Other sulphides were compared with the sphalerite, in order to obtain inter-mineral fractionations for each specimen. This method eliminates errors arising out of drift in real or apparent S^{32}/S^{34} ratio in the standard gas between analyses of components of an assemblage.

c) Calculations

The S^{32}/S^{34} ratio for each sample is expressed relative to the sulphur isotope ratio for meteorite sulphur (which is generally accepted to be 22.22 (Jensen and Dessau, 1967)) as a δS^{34} value, defined as :

$$\delta S^{34}_{\text{sample}} (\text{‰}) = \left[\left(\frac{S^{34}}{S^{32}} \right)_{\text{sample}} / \left(\frac{S^{34}}{S^{32}} \right)_{\text{meteorite}} - 1 \right] \times 10^3$$

The δS^{34} values, relative to Park City pyrite, are corrected for $S^{32}O^{16}O^{18}$ contribution to the mass 66 peak, to give δS^{34} values relative to meteorite sulphur, using the empirical equation :

$$\delta^{CDT} = 1.09 \delta^{PCP} + 4.05$$

where δ^{CLT} is the δS^{34} value relative to Canon Diablo Troilite
 δ^{PCP} is the raw data, relative to Park City Pyrite.

EXPERIMENTAL RESULTS

A) SAMPLE PURITY

The results of X-ray diffraction analyses of mineral concentrates are presented below in Table 1. The concentration of impurities was estimated from relative peak heights. All samples were run at high sensitivity, so that the detection limit is considerably less than 1 %. One drawback to this method is that sphalerite cannot be detected in pyrite concentrates, because of coincidence of peaks.

The trace of chalcopyrite in the Keymet sphalerite concentrate was determined, by examination of a polished section, to be due to exsolution blebs of chalcopyrite along crystallographic directions in the sphalerite. Although all Dundas pyrite samples were selected from crystals showing pyrite morphology, a large proportion of marcasite is evident. This is presumably due to fine grained intergrowths or to marcasite pseudomorphs of pyrite.

B) MANGANESE ANALYSES

The data from the neutron activation work is presented in Table 2. Comparison of liquid and steel standards showed a consistent deviation from the expected values. This could be overcome by assuming either a value of 6000 ppm (as compared to 5440 ppm) for the steel standard, or a lower value for the liquid standard than was calculated. Because relative concentrations are most important in determining partition coefficients, and because the NBS steel is an accepted standard, the standards were adjusted for consistency, relative to the NBS steel. This produces a 10% decrease relative to concentrations

TABLE 1 - Purity of samples as determined by X-ray diffraction

<u>Sample</u>	<u>Primary Mineral</u>	<u>Impurities</u>
KG-1	galena	pure +
KS-1	sphalerite	1-2 % galena trace of chalcopyrite
KP-1	pyrite	pure
KCpy-1	chalcopyrite	unidentified trace
KC-1	calcite	pure
KG-2	galena	pure
KS-2	sphalerite	pure
KP-2	pyrite	pure
KC-2	calcite	pure
K-2 matrix	sericite	1% pyrite, 1% quartz
DG-1	galena	pure
DS-1	sphalerite	pure
DP-1	pyrite	~40% marcasite
DC-1	calcite	pure
D-1 matrix	sphalerite	pure
DG-2	galena	pure
DS-2	sphalerite	pure
DP-2	pyrite	~40% marcasite
DC-2	calcite	pure

+ impurities below background level, ie <1%

TABLE 2 Manganese concentrations in coexisting sulphides (corrected for consistency with National Bureau of Standards steel 19G = 5440 ppm Mn).

<u>Sample</u>	<u>Minerals</u> (concentration of Mn in ppm)				
	<u>Galena</u>	<u>Sphalerite</u>	<u>Pyrite</u>	<u>Chalcopyrite</u>	<u>Calcite</u>
K-1	5.8 } 4.7 } ± 0.7 6.6 }	4410 } + 300* 4460 }	130 ± 15	106 ± 10	8380 ± 400
K-2	12.0 } ± 1.5 15.9 }	3480 } ± 250 3510 }	31 ± 5	-	15,300 ± 700 ⁺⁺
D-1	0.31 ± 0.2	40.0 } ± 5.0 39.8 }	12.2 ± 1.0	-	305 } 305 } ± 25 ⁺ 350 }
D-2	0.20 ± 0.1	44.5 } ± 5.0 18.0 }	11.0 ± 1.0	-	644 } ± 50 ⁺ 644 }

Note: Replicate analyses represent separate experiments, using new standards and samples, except :

- + sample compared with liquid and steel standards, same experiment
- ++ sample compared with 2 steel standards, same experiment
- * different samples compared with the same standard

obtained by taking 6000 ppm as the value for the steel. This discrepancy could be due to impurities in the Specpure MnO_2 (unlikely), or to errors in preparation of the standard.

C) SULPHUR ISOTOPES

The corrected $\delta^{CDT}S^{34}$ values for the sphalerite in each sample are presented in Table 3. Inter-mineral fractionation values,

Δ_{ab} , where :

$$\Delta_{ab} = 10^3 \ln \left[\frac{(S^{34}/S^{32})_a}{(S^{34}/S^{32})_b} \right]$$

$$\approx \delta S^{34}_a - \delta S^{34}_b$$

are given in Table 4. Each value represents a separate determination, by direct comparison of the mineral pair, using the same SO_2 samples.

TABLE 3 δS^{34} values of sphalerite

<u>Sample</u>	<u>$\delta^{CDT}S^{34}$</u>	<u>Average for Deposit</u>
KS-1	0.30	0.12 \pm 0.18
KS-2	-0.06	
DS-1	27.63	27.51 \pm 0.4
DS-2	27.08	
DS-3	27.81	

TABLE 4 Δ_{ab} (‰) values (all ± 0.1 ‰)

Sample	Δ_{SG}	Δ_{PG}	Δ_{PS}	Δ_{SCpy}
K-1	1.45 } 1.47 1.48 }	1.66 } 1.76 1.86 }	0.43 } 0.22 0.0 }	-0.05
K-2	0.87	0.72	-0.22	-
D-1	3.62 } 3.60 3.58 }	3.82	+0.11 } 0.0 -0.10 }	-
D-2	4.87	5.96	0.80	-
D-3	3.60	2.98 ⁺	-0.62	-

+ calculated from other mineral pairs

DISCUSSION

A) PRECISION AND ACCURACY IN MANGANESE ANALYSES

The radioactive decay process involves a statistical error which is equal to the square root of the number of counts, because it is a first order rate reaction (ie $dN/dt \propto N$). Since peak heights varied from about 100 to 1000 counts per channel, the resulting uncertainty varied from 10% to 3%. Additional errors are added by weighing of samples and standards, uncertainty of standard concentrations and uncertainty of calculated peak areas. Thus the overall uncertainty ranges from about 5 to 12%, depending on the sample. These values are shown in Table 2.

The determination of manganese in the Dundas galenas involved several additional sources of error :

a) The acid used to make up the standards contributed about 50% of the standard manganese activity. Although this is automatically subtracted during counting, some error will be introduced by decay during the interval between counting of blank and standard.

b) The permanganate determination gave a yield of $107 \pm 1\%$ for the chemical procedure. (All yields were therefore assumed to be 100%) This reflects the size of the uncertainty in these manganese analyses.

The overall uncertainty in the Dundas galena values is, therefore, probably 30% or more.

An additional source of error occurs in samples with a high Fe/Mn ratio, due to the reaction (during irradiation) :



which results in an increase in the apparent manganese

concentration. This error cannot be precisely corrected for, at present, because of uncertainty as to the cross section (ie probability) of the reaction. An estimated value has been used in Appendix 1 to calculate the approximate magnitude of the error.

B) THE MnS GEOTHERMOMETER

The theory and application of the distribution of manganese between coexisting sulphides is discussed by Bethke and Barton (1971). Several of their conclusions are significant for this study :

- 1) Application of the method requires equilibrium crystallization of sulphides, with subsequent freezing in of compositions.
- 2) Temperature results are almost independent of pressure, since the compressibilities of sulphides are quite low, in general.
- 3) Incomplete separation of the galena and sphalerite tends to raise the apparent equilibrium temperature, by reducing the apparent fractionation. This effect is illustrated in Figure 4.

The geothermometer is based on the equilibrium distribution of manganese between galena and sphalerite, so that the activity is the same in both phases :

$$a_{\text{MnS}}^{\text{S}} = a_{\text{MnS}}^{\text{G}} = a_{\text{MnS}}^{\text{soln}}$$

that is, the activities of MnS in sphalerite, galena, and the solution from which they form, are equal. This activity is related to mole fraction, N , by the activity coefficient :

$$N_{\text{MnS}}^{\text{S}} = a_{\text{MnS}}^{\text{S}} / \gamma_{\text{MnS}}^{\text{S}}$$

The activity coefficient is an inverse measure of the ability of the host phase to accommodate the manganese.

The distribution coefficient, K , which is the ratio of the

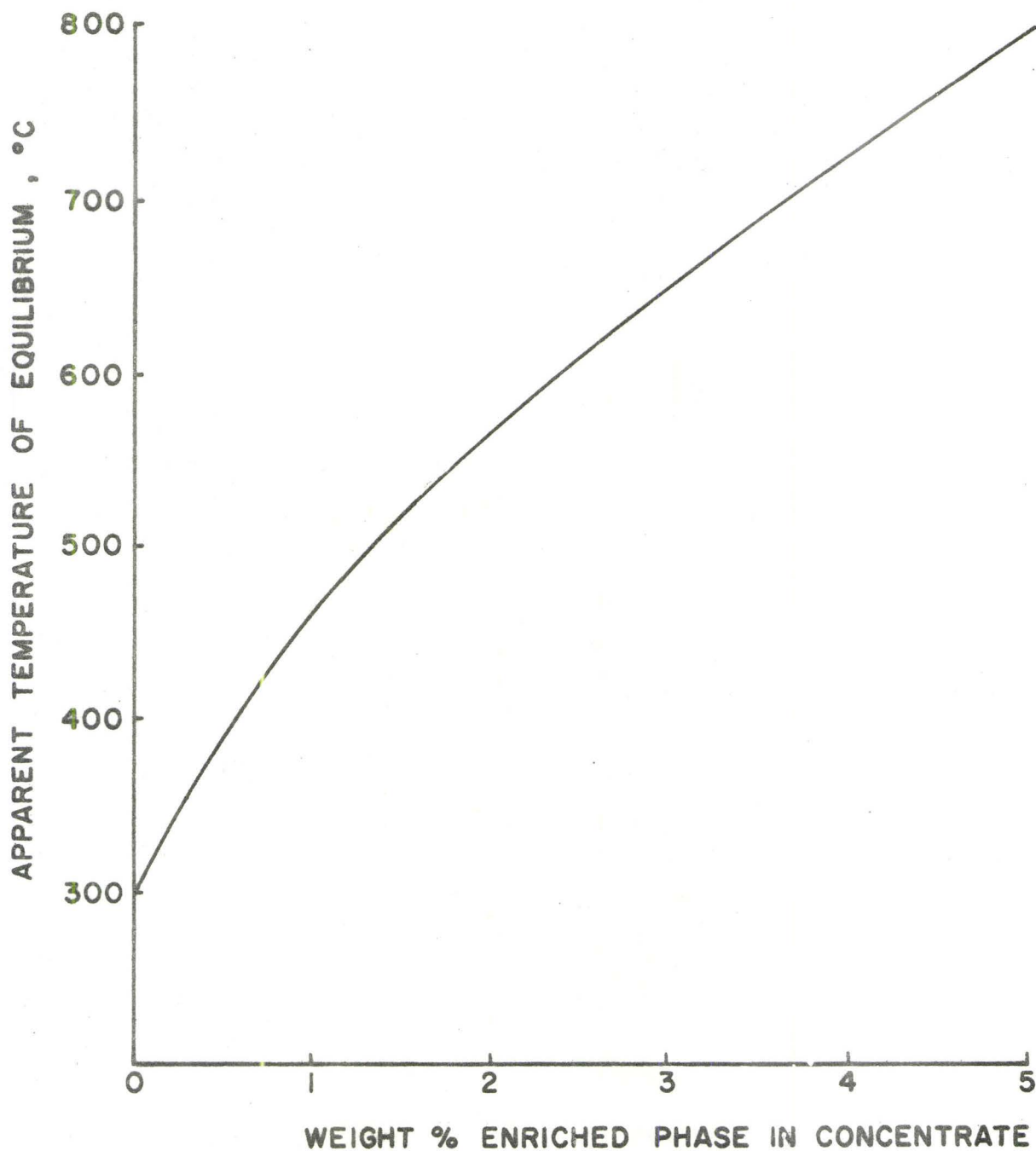


Figure 4 Effect of contamination of galena by sphalerite (after Bethke and Barton, 1971), assuming an equilibrium temperature of 300°C

concentrations of MnS in sphalerite and galena, may be written :

$$K_{\text{MnS}}^{\text{SG}} = N_{\text{MnS}}^{\text{S}} / N_{\text{MnS}}^{\text{G}} = \gamma_{\text{MnS}}^{\text{G}} / \gamma_{\text{MnS}}^{\text{S}}$$

Fortunately, the activity coefficients vary only slightly with pressure, and in the same sense, so that the small effect almost cancels out when the ratio, K, is considered.

The effect of temperature on the distribution coefficient is expressed as :

$$\frac{d \log K}{d(1/T)} = \frac{-\Delta \bar{H}}{2.3R}$$

where $\Delta \bar{H}$ is the difference in the partial molar enthalpies of the reactants and products of the distribution reaction (ie $\bar{H}_{\text{MnS}}^{\text{S}} - \bar{H}_{\text{MnS}}^{\text{G}}$). The graph of this relation is reproduced as Figure 5. It should be noted that Bethke and Barton used an X-ray diffraction technique to determine compositions which were much higher in MnS. In fact, their galena-sphalerite-MnS experiments involved a four-phase equilibrium between galena, sphalerite, wurtzite and alabandite (MnS). This may introduce uncertainties in the applicability of MnS fractionations at low concentrations. The extrapolation to low temperatures, as discussed in the introduction, may also lead to additional uncertainties.

In order to apply the fractionation data of this study, without further investigations, we must assume that :

a) equilibrium was attained and frozen in. This could be checked by using other minor element geothermometers (eg. CdS in galena and sphalerite).

b) mineral concentrates are pure and homogeneous, that is, free from fluid inclusions, adsorbed films, mechanical mixtures, exsolved phases, and zonation. Although the X-ray diffraction work can verify some of these assumptions, others must be studied by microscope

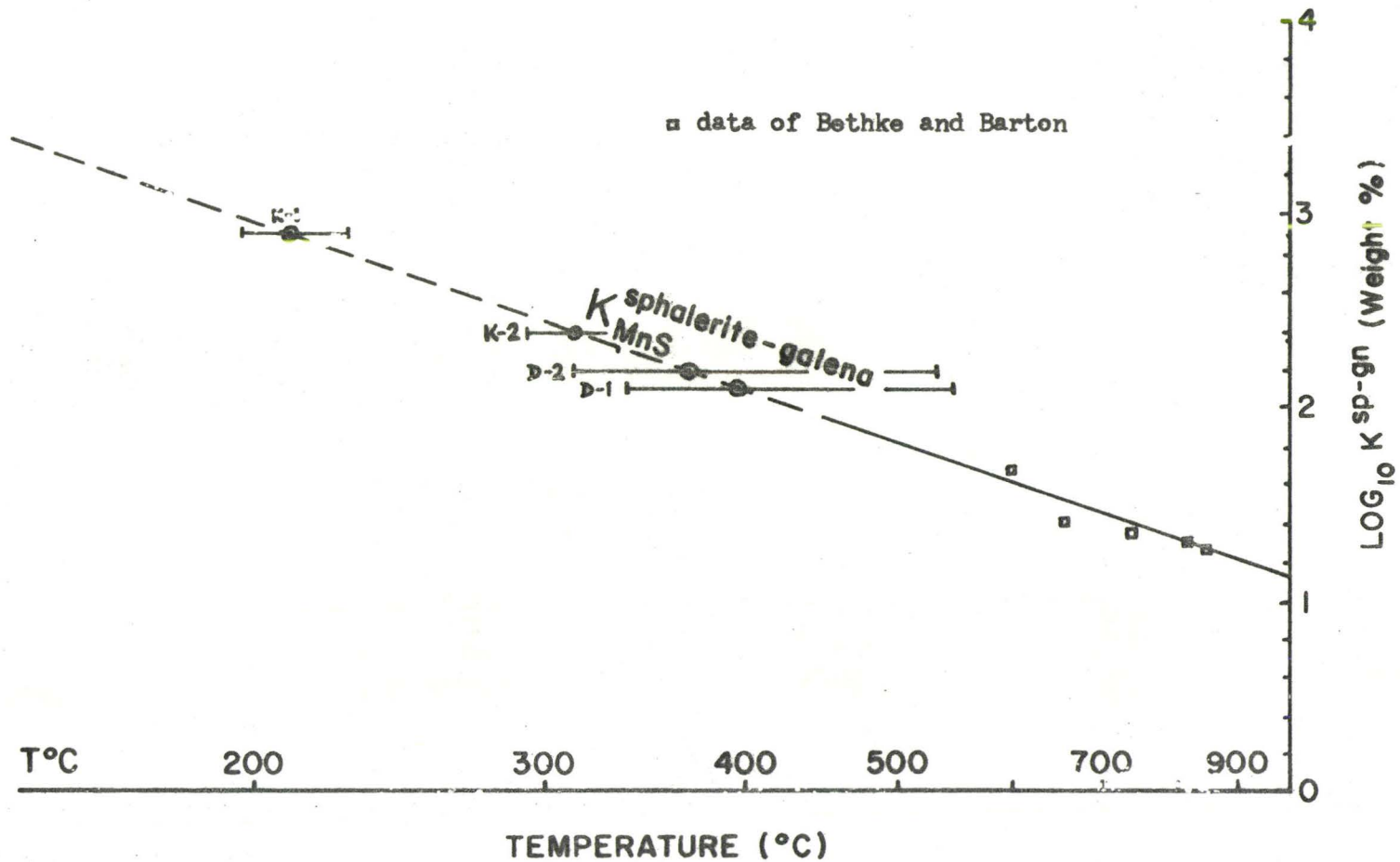


Figure 5 MnS Geothermometer (after Bethke and Barton, 1971)

Error bars represent uncertainty due to experimental error in Mn analyses.

(for fluid inclusions), leaching experiments (for adsorbed films), and possibly by electron microprobe (for zonation). For the present, it will be assumed that, if these contaminants are present, their effect is negligible relative to the experimental uncertainties of the method.

The assumption of equilibrium can also be checked by textural evidence. In the present study, the galena and sphalerite appear to have crystallized simultaneously, after pyrite and prior to calcite. Consequently, it is possible that equilibrium occurred between some phases, but not others, in the same sample. It is also possible that phases could be in textural disequilibrium but in chemical equilibrium, due to solid-state reactions.

The temperature results obtained from the MnS analyses are given in Table 5 and in Figure 5. The large range in temperatures for Dundas is due to the error in the galena values. It could be noted that a temperature of 200°C would result in a galena value of about 0.04 ppm MnS (40 ppb), assuming 40 ppm Mn in the sphalerite. This is about the sensitivity limit of the present procedure.

TABLE 5 Temperature results from the MnS geothermometer.

<u>Sample</u>	<u>Sphalerite</u> (ppm Mn)	<u>Galena</u> (ppm Mn)	K^{SG} +	<u>T(°C)</u>	<u>Range(°C)</u> ++
K-1	4440 ± 300	5.7 ± 0.7	780 ± 150	310	195 - 225
K-2	3500 ± 250	14.0 ± 1.5	250 ± 50	310	290 - 330
D-1	40 ± 5	0.31 ± 0.2	130 ± 80	400	340 - 540
D-2	31 ± 5	0.20 ± 0.1	155 ± 100	370	310 - 525

+ $K^{SC} = (\text{weight \% MnS in ZnS} / \text{weight \% MnS in PbS})$

++ Range of values due to experimental error in manganese analyses.

C) SULPHUR ISOTOPES

The sulphur isotope geothermometer is based on the fractionation of the sulphur isotopes, S^{32} and S^{34} , between coexisting sulphide minerals. These fractionations, given by :

$$\Delta_{ab} = (S^{34}/S^{32})_a / (S^{34}/S^{32})_b$$

are generally quite small, ranging from 1.000 to 1.005. These fractionations occur, for example, when galena and sphalerite crystallize at isotopic equilibrium, thus undergoing the isotopic exchange reaction:



for which the equilibrium constant $K^{SG} = \Delta_{SG}$. Urey (1947) and Bigeleisen and Mayer (1947) have shown that K should vary approximately as :

$$\ln K^{SG} = a_{SG} \cdot T^{-2}$$

where a_{SG} is a constant and T is the absolute temperature. It can be shown that, for $\delta S_S^{34} - \delta S_G^{34} = 5\text{‰}$:

$$\Delta_{SG} = 10^3 \ln K^{SG} \approx \delta S_S^{34} - \delta S_G^{34}$$

Thus Δ_{SG} , the fractionation, should be directly proportional to T^{-2} . This has been experimentally verified by Grootenboer and Schwarcz (1969), Rye and Czamanske (1969) and Kajiwarra and Krouse (1970) with the possible exception of pyrite-sulphur fractionations, which Grootenboer and Schwarcz report as lying on a curve of the form $\Delta_{ab} = a \cdot T^{-n}$, where $n \approx 3$.

TABLE 6 Temperature results from sulphur isotopes

<u>Sample</u>	$\Delta_{34S}(\text{‰})$	<u>A(°C)</u> ¹	<u>B(°C)</u> ²	<u>Average</u>	<u>Range</u> ³
K-1	1.47 ± 0.1	375 ± 25	460 ± 40	525	350 - 780
K-2	0.87 ± 0.1	560 ± 60	700 ± 80		
D-1	3.60 ± 0.1	150 ± 5	200 ± 10	150	85 - 210
D-2	4.87 ± 0.1	90 ± 5	130 ± 5		
D-3	3.60 ± 0.1	150 ± 5	200 ± 10		

¹ from curve of Grootenboer and Schwarcz (1969)

² from curve of Kajiwara and Krouse (1970)

³ range includes uncertainty of temperature results,

ie minimum = lowest temp. result minus its uncertainty

maximum = highest temp. result plus its uncertainty.

TABLE 7 Comparison of temperatures from the two geothermometers

<u>Sample</u>	<u>MnS fractionation</u>	<u>Sulphur Isotopes</u> ¹
K-1	210 ± 15 °C	420 ± 40 °C ²
K-2	310 ± 20	630 ± 70
D-1	400 $\begin{matrix} + 140 \\ - 60 \end{matrix}$	175 ± 25
D-2	370 $\begin{matrix} + 150 \\ - 60 \end{matrix}$	110 ± 20
D-3	-	175 ± 25

¹ These temperatures represent the average of the results obtained from the two curves - Grootenboer and Schwarcz (1969) and Kajiwara and Krouse (1970).

² This uncertainty represents the difference between each of the two temperature results, and their average.

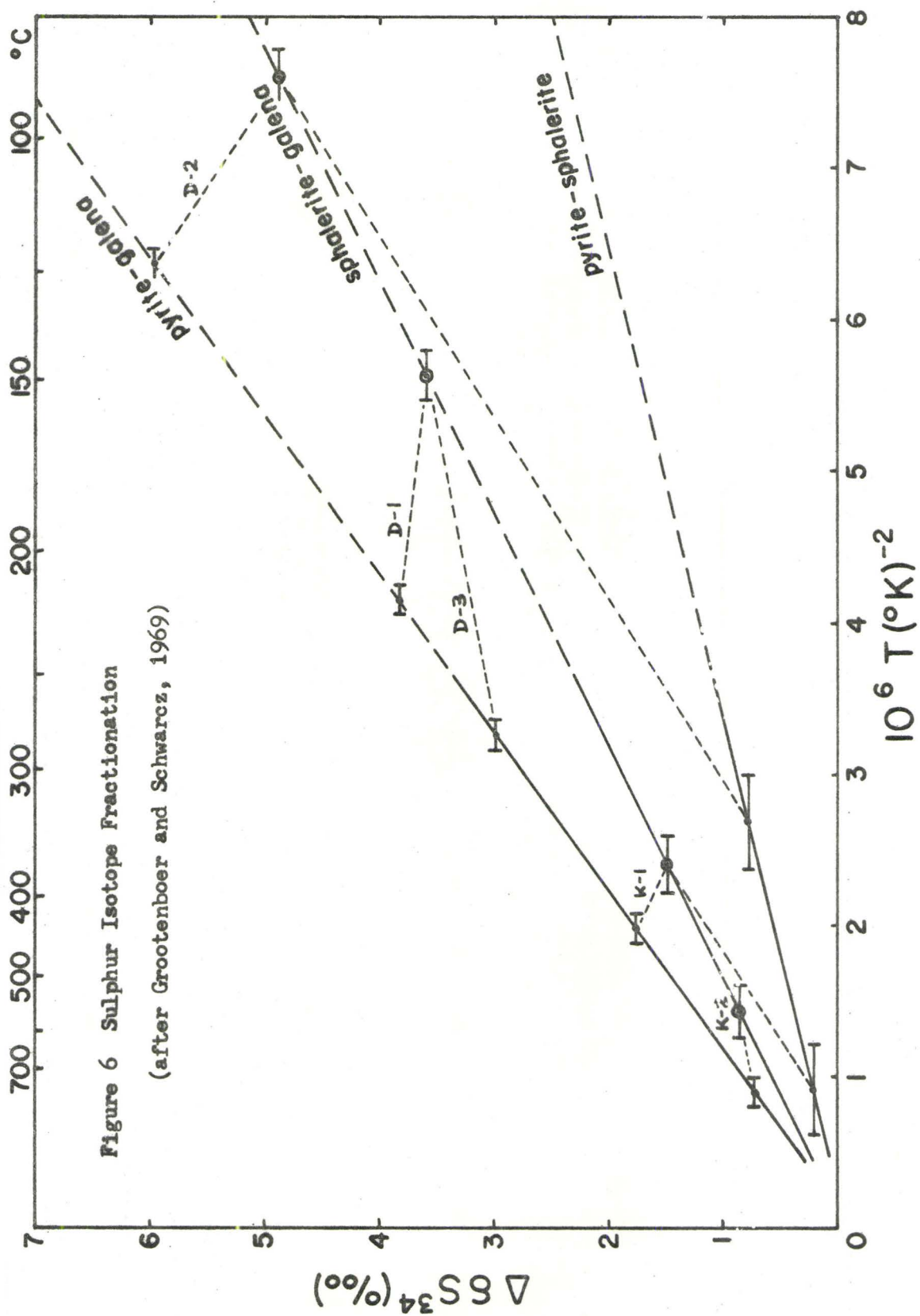
The precision of δS^{34} values appears to be about $\pm 0.05\%$, based on the reproducibility of the measurements. This results in a $\pm 0.1\%$ uncertainty in Δ_{ab} . Figure 6 shows the fractionation curves of Grootenboer and Schwarcz (1969) and the temperature results of this study. Figure 7 shows the same data on Kajiwara and Krouse's (1970) plot. The experimental work of Rye and Czamanske (1969) has produced a galena-sphalerite fractionation curve which is between the aforementioned curves.

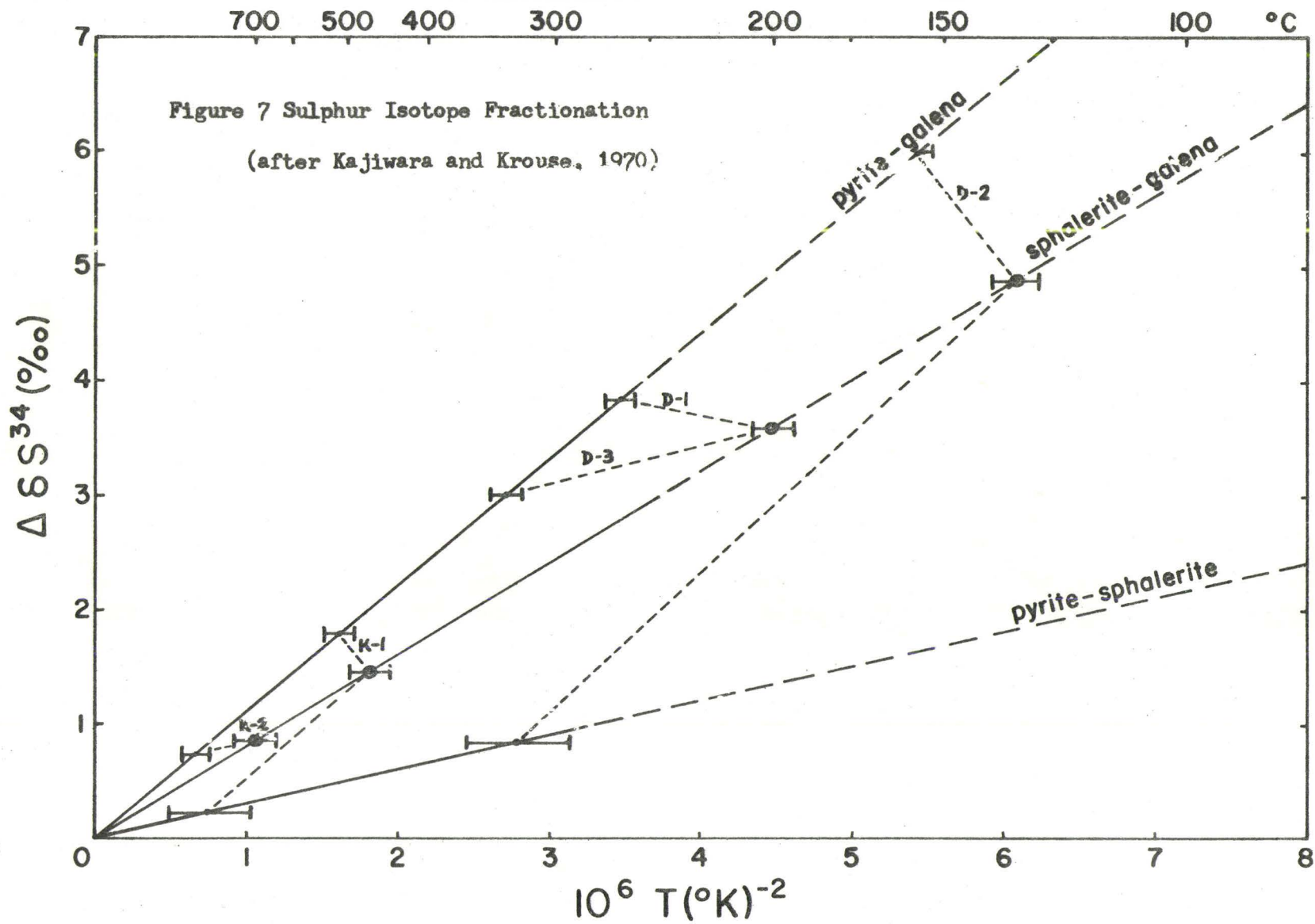
The consistently higher temperature values for pyrite-galena fractionation, and the negative values for pyrite-sphalerite fractionation, indicate that the pyrite was not in equilibrium with the galena and sphalerite, thus supporting the textural evidence. For the present, it is assumed that the sphalerite-galena fractionation represents (at least) a closer approach to equilibrium, and hence these temperatures are more reliable. These temperatures (see Table 6) represent an average of the galena-sphalerite curves in Figures 6 and 7. The uncertainty in these values is rather large, partly due to the differences in the temperature curves.

D) COMPARISON OF TEMPERATURE RESULTS

a) Yeymet

The temperature of equilibration of sulphur isotopes in this deposit appears to be about 525°C . Several temperature results have been obtained for this deposit by other methods. Roy (1961) points out that exsolution of chalcopryrite from sphalerite and tetrahedrite from (primary) chalcopryrite puts restrictions on the minimum temperature at which the ores could have formed. According to Buerger (1934),





chalcopyrite unmixes from sphalerite at 350 to 400°C. Edwards (1946) reports that tetrahedrite exsolution occurs at about 500°C. These represent maximum temperatures based on the assumption of saturation with Cu (in the sphalerite) and Sb (in the chalcopyrite). The presence of primary chalcopyrite and tetrahedrite(?) in the ores suggests that this saturation occurred, but the uncertainty as to the paragenetic sequence prevents the assertion that saturation of the ore solution occurred when the sphalerite and chalcopyrite were forming. Thus, it appears that crystallization of sulphides occurred at about 525°C, and that exsolution occurred as a solid state reaction during cooling.

The MnS fractionation data suggest an average temperature of $260 \pm 70^\circ\text{C}$ for equilibration of manganese in sulphides. If exsolution can occur at 350°C, it may not be unreasonable for chemical equilibria to remain unfrozen until 300°C or less.

Other facts which may have some bearing on the temperature of formation are :

a) wallrock alteration consists of sericite, quartz, and pyrite (see Table 1), as well as chlorite (McAllister, 1960)

b) stratiform deposits in the Ordovician rocks to the south give sulphur isotope temperatures of 350 - 450°C (Lusk and Crocket, 1969) Although it is generally accepted that these deposits are genetically related to the fissure deposits (based on mineralogy and other evidence) the nature of the relationship is uncertain.

c) Although generally discredited, the sphalerite geothermometer was used by Benson (1960) to give temperatures of 400 - 425 °C for the massive sulphide deposits.

b) Dundas

The temperature of equilibration of sulphur isotopes in this deposit appears to be about 150°C. Although no other data are available for this deposit, several estimates have been given for similar Mississippi Valley type occurrences. Roedder (1967) has reported values of 100 - 150°C based on fluid inclusion work. Campbell (1967) suggests temperatures in excess of 150°C, based on the melting point of hydrocarbons found in the ore at Pine Point, Northwest Territories. Thus the value of 150°C is quite acceptable, based on previous estimates.

The temperature result from the MnS fractionation is about 390°C. This appears to be too high, probably due to analytical error in the galena analyses, or to chemical disequilibrium. Another possibility is contamination - Roedder (1967) has reported fluid inclusions from Illinois containing 0.4% Mn. Small cavities, which may have been fluid inclusions, were noted in some of the galena. It was hoped that the crushing and acid leaching would remove such contaminants, but this may not have been effective.

E) ORIGIN OF THE DEPOSITS

a) Keynet

The δS^{34} value for this deposit appears to be very close to 0.0‰, since the sphalerite and pyrite average about +0.2‰, and the less abundant galena averages -1.4‰. This is consistent with the results of Tupper (1960) who reported an average S^{32}/S^{34} ratio of $22.22 + 0.025$, i.e. $\delta S^{34} = 0.0‰$. Sulphur of this isotopic composition is generally considered to be of magmatic hydrothermal origin (Jensen, 1967). A suitable model is, therefore, transportation of metals in

hydrothermal solution, possibly as bisulphide complexes (Barnes, 1967), with deposition occurring due to decreased pH, oxidation, loss of pressure, or dilution by groundwater.

b) Dundas

The δS^{34} value for this deposit is about +27.5‰. The presence of evaporite deposits in the overlying Salina formation of Devonian age suggest a possible source of the sulphur, since Devonian evaporites are reported (Holser and Kaplan, 1966) to range in δS^{34} values from 15 to 30‰. The resulting sulphate in the solution or brine could be reduced to sulphide by bacterial action (Jensen and Dessau, 1967) or by reduction with organic materials including petroleum hydrocarbons or methane (Barton, 1967). The main problem appears to be in reducing $SO_4^{=}$ to $S^{=}$ without inducing a large kinetic isotope effect, since the original $SO_4^{=}$ could not have been much heavier than $\delta S^{34} = 30‰$. Both methods can be expected to produce only small effects under the right conditions. For example, Kemp and Thode (1968) have found that, in bacterial reduction, the nature of the electron donor affects the isotopic fractionation, and that high metabolic rates substantially reduce the resulting fractionation. Similarly, a high reaction rate would reduce the fractionation resulting from reduction by organic materials. Either method would produce small fractionations if the reduction occurred in an almost-closed system. It should be noted that tar (or pyrobitumen) occurs in small amounts at Dundas, although a direct relation to sulphides is not apparent.

Comparison of Dundas and Pine Point

Studies of the Pine Point area by Jackson and Folinsbee (1969) Sasaki and Krouse (1969) and others, indicate a number of similarities. In particular, the sulphur isotope data are of some interest. Sasaki and Krouse report an overall Δ_{SG} value of 3.5‰ (cf. 4.0‰ for Dundas). Their δS^{34} values are commonly in the sequence $\delta_{sl} \geq \delta_{py} > \delta_{gn}$, as at Dundas, whereas the theoretical order should be $\delta_{py} > \delta_{sl}$. They suggest that this is due to disequilibrium. Although their δS^{34} value for the deposits (~20‰) is somewhat lower than the Dundas value (27.5‰), both are consistent with a Devonian evaporite source.

The paleogeographical setting of the deposits is also similar - Pine Point being located in the dolomitic Presquile Barrier Reef at the edge of the Elk Point Evaporite Basin, while the Dundas sulphides are in a dolomitic reef, the Guelph-Lockport formation, at the edge of the Michigan evaporite basin.

CONCLUSIONS

1) The sulphur isotope data suggest that galena and sphalerite equilibrated in both sulphide deposits, since the temperature results are reasonable. Pyrite did not equilibrate, as seen by both textural and isotopic evidence.

2) Applicability of the sulphur isotope geothermometer to low temperature deposits is presently restricted by uncertainty in calibrating the fractionation with respect to temperature (but appears to give more reasonable results than the MnS geothermometer, using present techniques).

3) Applicability of the MnS geothermometer to low temperature galena-sphalerite assemblages of the Mississippi Valley type cannot be evaluated until analytical errors for low level Mn determination in galena can be improved and possible error due to fluid inclusions eliminated.

SUGGESTIONS FOR FURTHER STUDY

1) The precision in determination of low manganese contents could be improved by identifying specific interferences (by determining half-lives of interfering radionuclides) and developing a procedure for chemical separation.

2) The HCl used for making standards could be purified by distillation.

3) Longer irradiation and counting times could be used to increase the Mn^{56} activity, and thus to reduce the statistical error associated with the radioactive decay.

4) The electron microprobe analyser could be used to investigate zoning, particularly in sphalerite, where trace element concentrations are relatively high. Presence of zoning, especially of manganese, would indicate that sub-solidus re-equilibration did not occur extensively.

5) Cadmium could be studied in conjunction with manganese, to test for concordancy of temperature results (see Bethke and Barton, 1971).

6) The effect of Fe on Mn^{56} activity (Appendix 1) should be further investigated. A sample of iron (not necessarily Mn-free) could be wrapped in cadmium foil before irradiation. This shields the sample from thermal neutrons, which produce the $Mn^{55}(n,\gamma)Mn^{56}$ reaction. The resulting Mn^{56} activity would thus be due to the $Fe^{56}(n,p)Mn^{56}$ reaction, assuming no cobalt is present, so that a conversion factor could be determined for the Fe^{56} contribution (ie x% Fe \rightarrow y ppm Mn). This factor would vary, depending on the reactor flux, energy spectrum, and sample position, so that several experiments would have to be run.

BIBLIOGRAPHY

- Barnes, H.L. (1967) Sphalerite solubility in ore solutions of the Illinois-Wisconsin district. Econ. Geol. Mon. 3, ed. J.S. Brown, 326-332.
- Barton, P.B., Jr. (1967) Possible role of organic matter in the precipitation of the Mississippi Valley ores. Econ. Geol. Mon. 3, ed. J.S. Brown, 371-378.
- Beards, R.J. (1967) Guide to the Subsurface Paleozoic Stratigraphy of Southern Ontario. Ont. Dept. of Energy and Resources Management, Paper 67-2.
- Benson, D.G. (1960) Application of sphalerite geothermometry to some northern New Brunswick sulphide deposits. Econ. Geol. 55, 818-826.
- Bethke, P.M. and Barton, P.B., Jr. (1971) Distribution of some minor elements between coexisting sulfide minerals. Econ. Geol., 66, 140-163.
- Bevington, P.R. (1969) Data Reduction and Error Analysis for the Physical Sciences, McGraw-Hill.
- Bigeleisen, J. and Mayer, M.G. (1947) Calculation of equilibrium constants for isotopic exchange reactions. J. Chem. Phys. 15, 261.
- Caley, J.F. (1961) Palaeozoic Geology of the Toronto-Hamilton Area, Ontario. Geol. Surv. Can. Memoir 224.
- Campbell, N. (1967) Tectonics, reefs and stratiform lead-zinc deposits of the Pine Point area, Canada. Econ. Geol. Mon. 3, ed. J.S. Brown, 59-70.
- Cotton, F.A. and Wilkinson, G. (1962) Advanced Inorganic Chemistry-A Comprehensive Text. Interscience, P. 699.

- Davies, J.L. (1966) Geology of Bathurst-Newcastle area, N.B., Geol. Min. Assoc. Canada (1966) Guidebook: Geology of Parts of Atlantic Provinces, 33-43.
- Friedlander, G., Kennedy, J.W. and Miller, J.M. (1964) Nuclear and Radiochemistry, 2nd ed., J. Wiley and Sons, P. 178.
- Greiner, H.I. and Potter, R.R. (1966) Silurian and Devonian stratigraphy northern New Brunswick. Geol. Min. Assoc. Canada (1966) Guidebook: Geology of Parts of Atlantic Provinces, 19-29.
- Grootenboer, J. and Schwarcz, H.P. (1969) Experimentally determined sulfur isotope fractionations between sulfide minerals. Earth and Planetary Science Letters, 7, 162-166.
- Heath, R.L. (1964) Scintillation Spectrometry, Gamma-ray Spectrum Catalogue. 2nd ed., vol 2, U.S. Atomic Energy Commission.
- Hillebrand, W.F., Lundell, G.E.F., Bright, H.A. and Hoffman, J.I. (1953) Applied Inorganic Analysis. J. Wiley, 2nd edition.
- Holden, N.E. and Walker, F.W. (1968) Chart of the Nuclides, Knolls Atomic Power Laboratory, U.S. Atomic Energy Commission.
- Holser, W.T. and Kaplan, I.R. (1966) Isotope geochemistry of sedimentary sulfates. Chem. Geol. 1, 93-135.
- Jackson, S.A. and Folinsbee, R.E. (1969) The Pine Point lead-zinc deposits, N.W.T., Canada - Introduction and Paleogeology of the Presqu'ile Reef. Econ. Geol. 64, 711-717.
- Jensen, M.L. (1967) Sulfur isotopes and mineral genesis. Geochemistry of Hydrothermal Ore Deposits, ed. H.L. Barnes. Holt, Rinehart, Winston, N.Y., 143-165.
- Jensen, M.L. and Dessau, G. (1967) The bearing of sulfur isotopes on the origin of the Mississippi Valley type deposits. Econ. Geol. Mon. 3, ed. J.S. Brown, 400-409.

- Kajiwara, Y. and Krouse, H.R. (1970) Sulfur isotope geothermometry: pyrite-pyrrhotite-chalcopyrite-galena-sphalerite systems. Abstract, Geol. Soc. Amer. Ann. Mtg., Milwaukee, Wisconsin.
- Kemp, A.L.W. and Thode, H.G. (1968) The mechanism of the bacterial reduction of sulphate and of sulphite from isotope fractionation studies. *Geochim. Cosmochim. Acta* 32.
- Kolthoff, I.M. and Sandell, E.B. (1952) *Textbook of Quantitative Inorganic Analysis*, MacMillan, 3rd edition, 67-68.
- Lusk, J. and Crocket, J.H. (1969) Sulfur isotope fractionation in coexisting sulfides from the Heath Steele B-1 ore body, New Brunswick, Canada. *Econ. Geol.* 64, 147-155.
- McAllister, A.L. (1960) Massive sulphide deposition in New Brunswick. *Bull. Can. Inst. Mining Met.*, 53, 88-98.
- Roedder, E. (1967) Environment of deposition of stratiform (Mississippi Valley-type) ore deposits, from studies of fluid inclusions. *Econ. Geol. Mon.* 3, ed. J.S. Brown, 349-362.
- Roy, J.C. and Hawton, J.J. (1960) Table of Estimated Cross Sections for (n, p) , (n, α) , and $(n, 2n)$ reactions in a fission neutron spectrum, Atomic Energy of Canada Limited.
- Roy, S. (1961) Mineralogy and paragenesis of lead-zinc-copper ores of the Bathurst-Newcastle district, New Brunswick., *Geol. Surv. Canada Bull.* 72.
- Rye, R.O. and Czamanske, G.K. (1969) Experimental determination of sphalerite-galena sulfur isotope fractionation and application to the ores at Providencia, Mexico. Abstract, Geol. Soc. Amer. Ann. Mtg., Atlantic City, New Jersey.

- Sasaki, A. and Krouse, H.R. (1969) Sulphur isotopes and the Pine Point lead-zinc mineralization. *Econ. Geol.* 64, 718-730.
- Smith, J.V. (1967) Powder Diffraction File. American Society for Testing and Materials.
- Thode, H.G., Monster, J. and Dunford, H.B. (1961) Sulfur isotope geochemistry. *Geochim. et Cosmochim. Acta*, 25, 159-174.
- Tupper, W.M. (1960) Sulfur isotopes and the origin of the sulfide deposits of the Bathurst-Newcastle area of northern New Brunswick. *Econ. Geol.* 55, 1676-1707.
- Urey, H.C. (1947) The thermodynamic properties of isotopic substances. *J. Chem. Soc.*, 562.
- Wanless, R.K. and Thode, H.G. (1953) A mass spectrometer for high precision isotope ratio determinations. *J. Sci. Inst.*, 30, 395-398.
- Young, H.D. (1962) *Statistical Treatment of Experimental Data*, McGraw-Hill, 64-76.

APPENDIX 1

THEORETICAL CONSIDERATIONS IN NEUTRON ACTIVATION ANALYSIS OF MANGANESE

The determination of manganese is based on the reaction of Mn^{55} with a neutron to produce Mn^{56} , in high energy states. This nuclide then decays by emission of gamma rays of characteristic energies, to a more stable low energy state. The most frequent transition results in a gamma-ray energy of 0.845 Mev (million electron volts). The half-life for this decay is 2.54 hours (Holden and Walker, 1968). The rate of emission of gamma rays is directly proportional to the amount of Mn^{56} , and hence Mn^{55} , in samples and standards. Hence, the amount of Mn^{55} ($Mn^{55} = 100\%$ of natural manganese) in the sample can be directly related to the amount in the standard, assuming :

- 1) both received the same neutron flux
- 2) absorption effects of the matrix are either negligible or equal in standard and sample.
- 3) competing reactions are negligible, or can be corrected for.
- 4) both sample and standard are counted in the same position relative to the detector.
- 5) both are counted on the same detector (Ge-Li or NaI-Th) using the same settings. Counting times may vary, since they can be corrected for decay (see Appendix 2).

Interferences in this procedure are of two types - other nuclides like Co^{59} and Fe^{56} can form Mn^{56} by competing reactions, and Mn^{55} can produce nuclides other than Mn^{56} by similar reactions. Table 8 gives the reactions involved, with their relative probabilities, or cross sections.

TABLE 8 Nuclear reactions involved in manganese determination.

<u>Nuclide</u>	<u>Abundance (%)</u>	<u>Reaction</u>	<u>Cross Section⁺</u>
Mn ⁵⁵	100	Mn ⁵⁵ (n, γ) Mn ⁵⁶	13.3 barns ⁺⁺
Mn ⁵⁵	100	Mn ⁵⁵ (n, p) Cr ⁵⁵	0.4 millibarns
Mn ⁵⁵	100	Mn ⁵⁵ (n, α) V ⁵²	0.13 millibarns
Mn ⁵⁵	100	Mn ⁵⁵ (n, 2n) Mn ⁵⁴	0.16 millibarns
Co ⁵⁹	100	Co ⁵⁹ (n, α) Mn ⁵⁶	0.23 millibarns
Fe ⁵⁶	91.66	Fe ⁵⁶ (n, p) Mn ⁵⁶	0.87 millibarns

⁺ for a fission neutron spectrum, after Roy and Hawton (1960)

⁺⁺ for a thermal neutron spectrum, after Holden and Walker (1968)

In order to correct for these competing reactions, the value of the thermal neutron cross section must be determined, based on published fission neutron cross sections. An approximate conversion can be made by considering the so-called cadmium ratio, which gives the proportion of fission (fast) neutrons in the total reactor flux. This value varies from about 0.1 to 0.03, depending on the neutron spectrum in the particular irradiation position used. Thus the maximum thermal neutron cross section will be about 0.1 times the fission neutron cross section.

It can be seen that the reaction of Mn⁵⁵ to produce Mn⁵⁶ has a probability about 10⁵ times greater than these competing reactions. The reaction of Mn⁵⁵ to produce nuclides other than Mn⁵⁶ will therefore be negligible because of its low probability. Also, both sample and standard manganese undergo the same reactions, so that the effects will cancel. The reaction involving Co⁵⁹ will also be negligible, because of low cobalt contents of the minerals being considered.

TABLE 9 Correction of Mn analyses for Fe⁵⁶ (n, p) Mn⁵⁶ contribution

<u>Sample</u>	<u>Fe⁵⁶ (wt%)</u>	<u>Mn (ppm)¹</u>	<u>Fe/Mn</u>	<u>Fe⁵⁶ cont.² (ppm)</u>	<u>Mn (ppm)³</u>	<u>Mn (ppm)⁴</u>
19G steel	90	6000	150	6	6000	6000
KP-1	42.6	130	3280	3.1	127	127
KP-2	42.6	31	13,750	2.9	28.1	28.0
DP-1	42.6	12	35,600	2.5	9.5	9.0
DP-2	42.6	11	38,700	2.5	8.5	8.0
KCpy-1	27.9	110	2540	2.1	108	108
KS-1	8	4440	18	1	4440	4440
KS-2	8	3500	23	1	3500	3500
DS-1	5	40	1250	1	40	40
DS-2	5	31	1600	1	31	31

¹ 1st approximation from activation analysis (= Mn⁵⁵+ Fe⁵⁶ contributions)

² Fe⁵⁶ contribution = (A/(A+1))Mn

where , A = (Mn⁵⁶ activity due to Fe⁵⁶/Mn⁵⁶ activity due to Mn⁵⁵)

= (Fe/Mn) x (0.1/13,300) x (55/56)

³ 2nd approximation

⁴ 3rd approximation

The reaction of Fe^{56} to produce Mn^{56} will be quite significant however, since the high proportion of iron in many of the samples tends to compensate for the low probability of interaction. An approximate thermal neutron cross section of 0.1 millibarns can be used to estimate the magnitude of the Fe^{56} contribution to the measured Mn^{56} activity. This has been done in Table 9, for samples containing large amounts of iron. The 'true' manganese content is calculated by successive approximations, by determining the ratio of Fe^{56} - and Mn^{55} -produced activities (activity = concentration x cross section). From these values, the Fe^{56} contribution can be determined, and then subtracted from the original Mn value to give a second approximation to the true Mn concentration. This new value is used to determine an improved Fe/Mn ratio, and the process is repeated.

The Fe content of the sphalerites is estimated from values reported by Benson (1960). It can be seen that the correction becomes significant (relative to experimental uncertainty) only when the Fe/Mn ratio is large - a ratio of 1300 produces a 1% correction, a ratio of 13,000 produces a 10% correction. The resulting error in sphalerites will not be great enough to significantly affect the temperature values, due to larger errors from other sources. The error in pyrite analyses, however, could be as great as 30% .

APPENDIX 2

CORRECTION OF COUNTING TIME FOR DECAY

When comparing samples with standards that have been counted for a different length of time, it is necessary to adjust the counting time assigned to each sample. This is because the decay rate (or counting rate) decreases during counting. Thus the number of counts accumulated after a certain length of time will not be twice the number of counts accumulated in half that time, unless the half-life is very long relative to the counting interval. In the same way, if two different samples are considered, the ratio of total counts for one sample relative to the other will change if the counting interval for one of the samples is changed.

The approach used to correct for this decay is to determine the time during the counting interval at which half of the counts has accumulated. This is illustrated in Figure 8. The area under any portion of the curve is the number of counts accumulated during that time interval. If we superimpose on the curve, a rectangle with the same area as the integrated curve, then the point of intersection of the curve and the horizontal line will be at the time at which half the total area has accumulated.

If these times, t'_1 and t'_2 , are plotted on a semilogarithmic graph with their corresponding average counting rate values, then the two points will lie on a line with a slope corresponding to the half-life of the isotope being counted. If the initial times, t_0 , or final times, t_1 and t_2 , were plotted in this way, the resulting points would not lie on a line with the appropriate slope.

The value of t' can be calculated for any counting interval, t_0 to t , by integrating the decay equation :

$$A = A_0 e^{-\lambda t} \quad \text{where } \lambda = \ln 2 / \text{half-life}(t_{1/2})$$

Since the area under the curve from t_0 to t' is equal to the area from t' to t , we can write :

$$\int_{t_0}^{t'} A_0 e^{-\lambda t} dt = \int_{t'}^t A_0 e^{-\lambda t} dt$$

Solving for t' , we get :

$$t' = - \ln \left(\frac{e^{-\lambda t} + 1}{2} \right) / \lambda$$

From this relation, it can be seen that :

- a) as (counting time/half-life) increases, $t'/t \rightarrow 0$
- b) as (counting time/half-life) decreases, $t'/t \rightarrow 1/2$

In the case of Mn^{56} , the half-life (2.54 hr) is much greater than the counting time (maximum 25 min), so that t' is close to the midpoint of the counting interval :

$$\text{if } t = 25 \text{ min, } t' = 12.1 \text{ min}$$

$$t = 10 \text{ min, } t' = 4.9 \text{ min}$$

$$t = 5 \text{ min, } t' = 2.5 \text{ min}$$

Thus the correction only becomes significant for long counting intervals (more than 10 min for Mn^{56}). To apply the correction the value of t' is added to the clock time, t_0 (when the count started), and the result, $t_0 + t'$, is used for comparing different samples at different times.

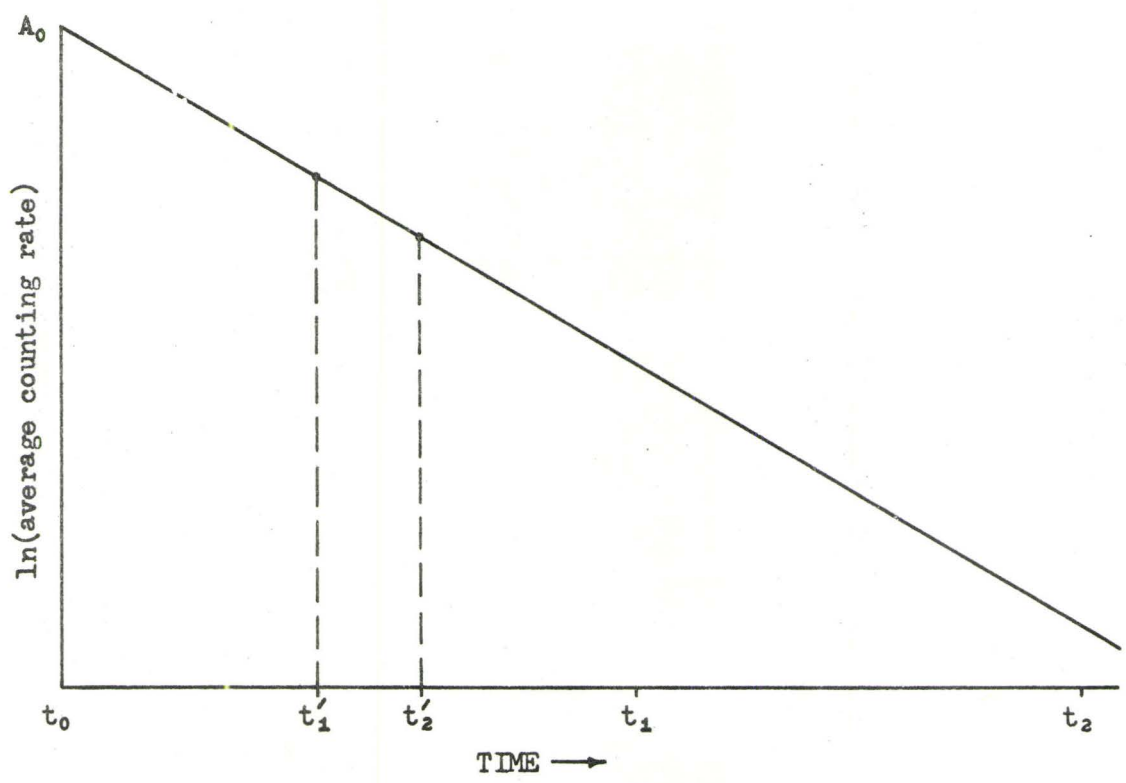
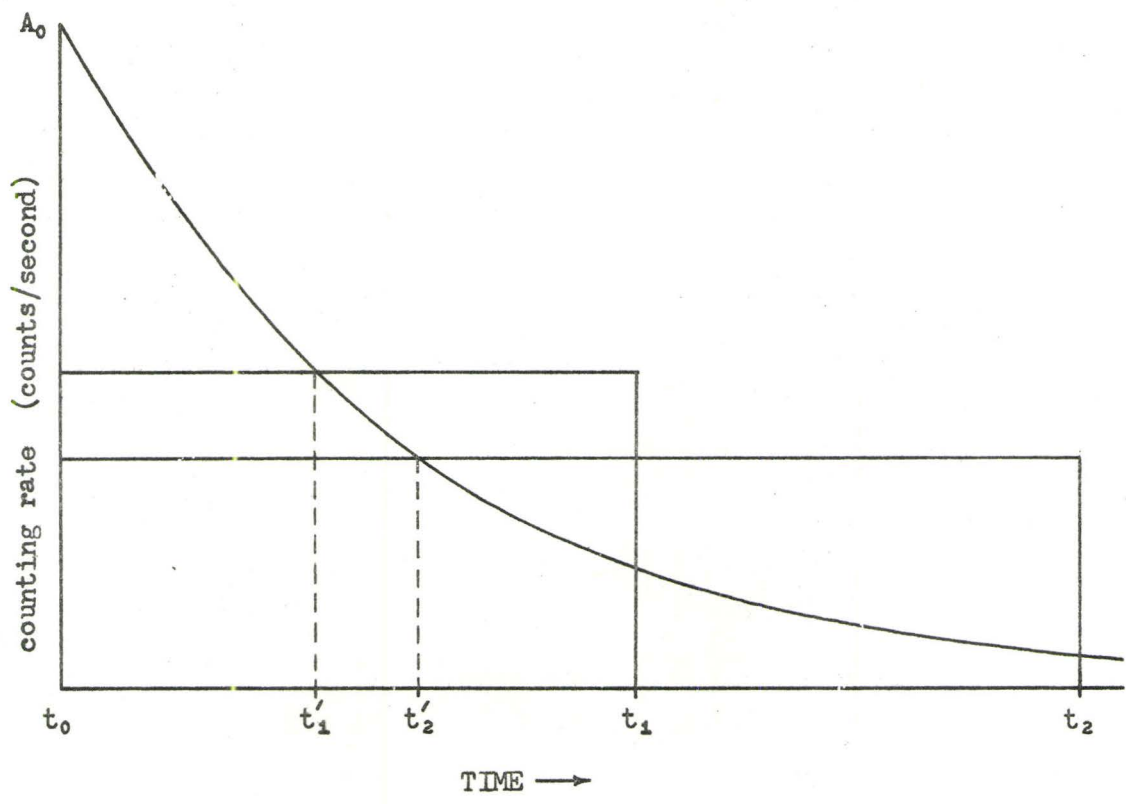


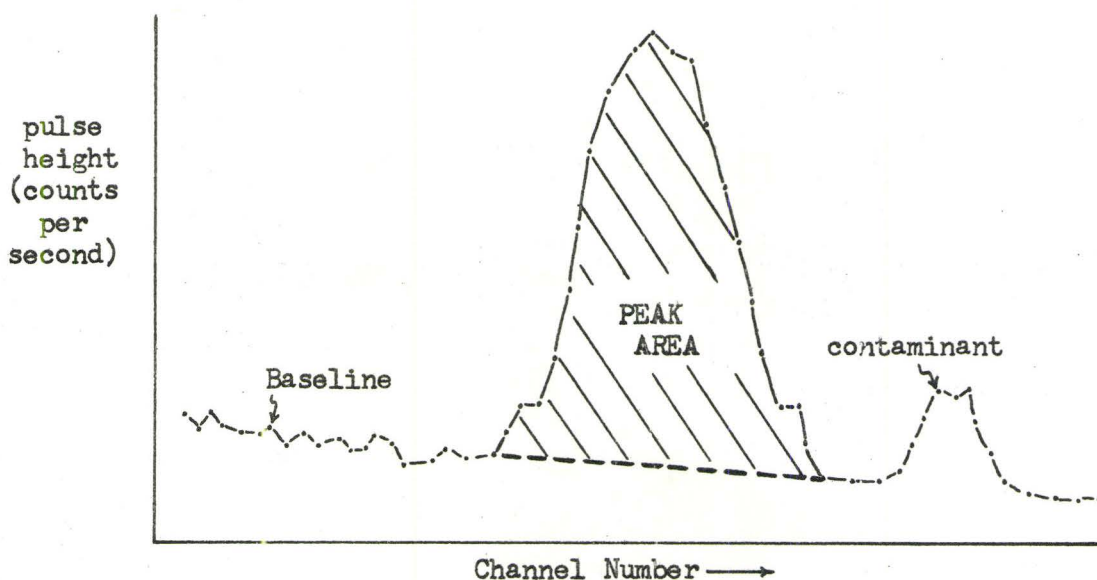
Figure 8 Graphical illustration of relationship between counting interval and time of accumulation of half the total counts.

APPENDIX 3

A FORTRAN IV COMPUTER PROGRAM FOR HANDLING γ -SPECTRUM DATA FROM NEUTRON ACTIVATION ANALYSIS

This program is designed to calculate the area under a sample peak, such as would be obtained from a multichannel γ -spectrum analyser.

A graph of the raw data might appear somewhat as follows :



The method used is to fit a polynomial to the baseline and a Gaussian function to the peak. The area under the peak can then be determined from the parameters of the fitted functions.

The baseline polynomial, of the form :

$$y = a_1 + a_2x + a_3x^2 + a_4x^3 + \dots$$

is fitted by a least-squares method to the baseline values, with the statistical error of each point being taken into account. This error, which is due to the probabilistic nature of radioactive decay, is equal to the square root of the number of counts, because it is a first order rate reaction, ie $dN/dt \propto N$. Hence, for each channel

number, x_i , the pulse height, y_i , has an error, $\pm\sqrt{y_i}$, associated with it. The statistical parameter, X^2 (chi-squared), is determined for the final polynomial as a measure of the goodness of fit. The definition of X^2 is :

$$X^2 = \sum_x (y_o - y_p)^2 / y_p$$

where y_o is the observed pulse height

y_p is the pulse height given by the polynomial

\sum_x is the sum over the channel numbers

The Gaussian function, which is the theoretical shape of the peak (see, for example, Friedlander et al, 1964), is defined as :

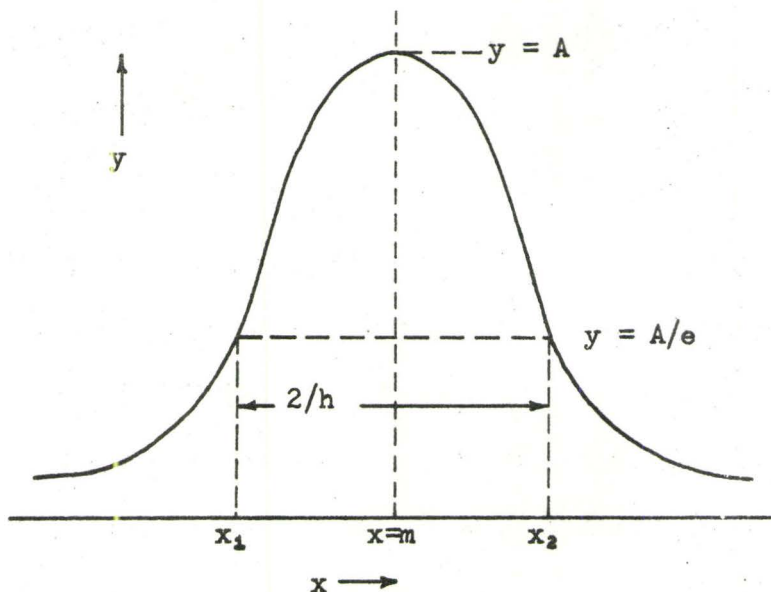
$$y = A \exp(-h^2(x - m)^2)$$

where A is the maximum value of y

m is the value of x where $y = A$, ie the centre of the symmetrical function.

h is an inverse measure of the width of the function,

so that : $2/h = \text{width at } A/e = (x_2 - x_1)$



The Gaussian function is fitted by determining the parameters A, h, and m, from the sample data - A is determined as the maximum y value, h is determined from the width, $x_2 - x_1$, and m is taken as the midpoint of the interval x_1 to x_2 .

PROCEDURE The program handles the data by the following steps:

1) INPUT

a) The sample name (10-digit alphanumeric) and range of channel numbers (5-digit integers) are read in, along with the first and last x values of three (and only three) regions which are treated as baseline (these must be in increasing order).

b) The pulse height values are read in from data cards, the first and last values being those specified by the range in part(a) above.

2) BASELINE SEPARATION

The x and y values of the specified baseline regions are extracted from the input data, and stored in a separate array.

3) FIT POLYNOMIAL TO BASELINE

The baseline polynomial is fitted to the data in the separated array, using a subroutine developed by Bevington (1969). The X^2 value is also determined at this stage.

4) SUBTRACT BASELINE

The baseline polynomial is subtracted from the input data to give a residual spectrum, in which the sample peak is sitting on a baseline of zero.

5) SMOOTH DATA

Because peaks are often jagged at the top, the maximum is best determined after one or more smoothings of the data. The smoothed

curve is obtained by computing a running mean: ($i = 1$ to N , $N =$ last x value)

$$y(i)_{\text{smooth}} = y(i-1)/4 + y(i)/2 + y(i+1)/4$$

$$y(1)_{\text{smooth}} = 3y(1)/4 + y(2)/4$$

$$y(N)_{\text{smooth}} = y(N-1)/4 + 3y(N)/4$$

It should be noted that smoothing does not significantly affect the peak area, although the shape of the curve is altered- the change in width compensating for the change in height.

The most suitable number of smoothings is best determined by trial and error. For no smoothing, the entire step 5 section is removed; for 1 smoothing, statements 20 and 9 are removed; for 2 or more smoothings, the last number in statement 20 specifies the desired number of smoothings.

6) LOCATE MAXIMUM OF PEAK

This portion of the program requires that the peak of interest be the highest peak in the data.

7) DETERMINE PEAK WIDTH

The values of x_1 and x_2 (see previous diagram) are determined by interpolation. These two x values are used to determine h and m .

8) DETERMINE PEAK AREA

The area under a Gaussian curve is given by $AREA = A\sqrt{\pi}/h$
(Young, 1962)

9) OUTPUT

- a) Sample name and range of channel numbers
- b) The input data
- c) The baseline polynomial and X^2
- d) The residual data, unsmoothed

- e) The residual data, smoothed
- f) The area
- g) OPTION: the Gaussian function which was used to determine the area
- h) OPTION: computer plots of the input data, and the unsmoothed and smoothed residual data.

EXAMPLE :

The following is an example of the input data, with the resulting output. The graphs have been omitted. The fitted function, and the affect of rounding are shown in Figure 9.

1st card:

KG-2 12.50 470 600 470 510 549 562 590 600

remaining cards:

given with output data.

AREA = 5680.71

GAUSS(X) FROM CHANNEL 523 , INCREMENT= .10

.18	.20	.22	.25	.27
.30	.34	.37	.41	.46
.51	.56	.62	.69	.76
.84	.92	1.02	1.12	1.23
1.35	1.48	1.63	1.78	1.96
2.14	2.34	2.56	2.80	3.06
3.34	3.64	3.96	4.31	4.69
5.10	5.54	6.02	6.53	7.07
7.66	8.29	8.97	9.70	10.47
11.30	12.19	13.14	14.15	15.23
16.38	17.60	18.90	20.28	21.75
23.30	24.95	26.70	28.54	30.50
32.56	34.74	37.03	39.45	42.00
44.68	47.50	50.46	53.56	56.81
60.22	63.78	67.51	71.40	75.46
79.70	84.11	88.70	93.48	98.44
103.59	108.93	114.47	120.19	126.12
132.24	138.55	145.06	151.77	158.68
165.78	173.07	180.55	188.22	196.07
204.10	212.31	220.68	229.22	237.92
246.78	255.77	264.90	274.16	283.54
293.03	302.62	312.29	322.04	331.85
341.72	351.62	361.55	371.50	381.43
391.36	401.25	411.09	420.87	430.57
440.17	449.66	459.03	468.25	477.31
486.20	494.89	503.38	511.64	519.66
527.42	534.91	542.12	549.03	555.62
561.88	567.81	573.38	578.59	583.42
587.87	591.92	595.57	598.81	601.63
604.03	606.00	607.54	608.64	609.30
609.52	609.30	608.64	607.54	606.00

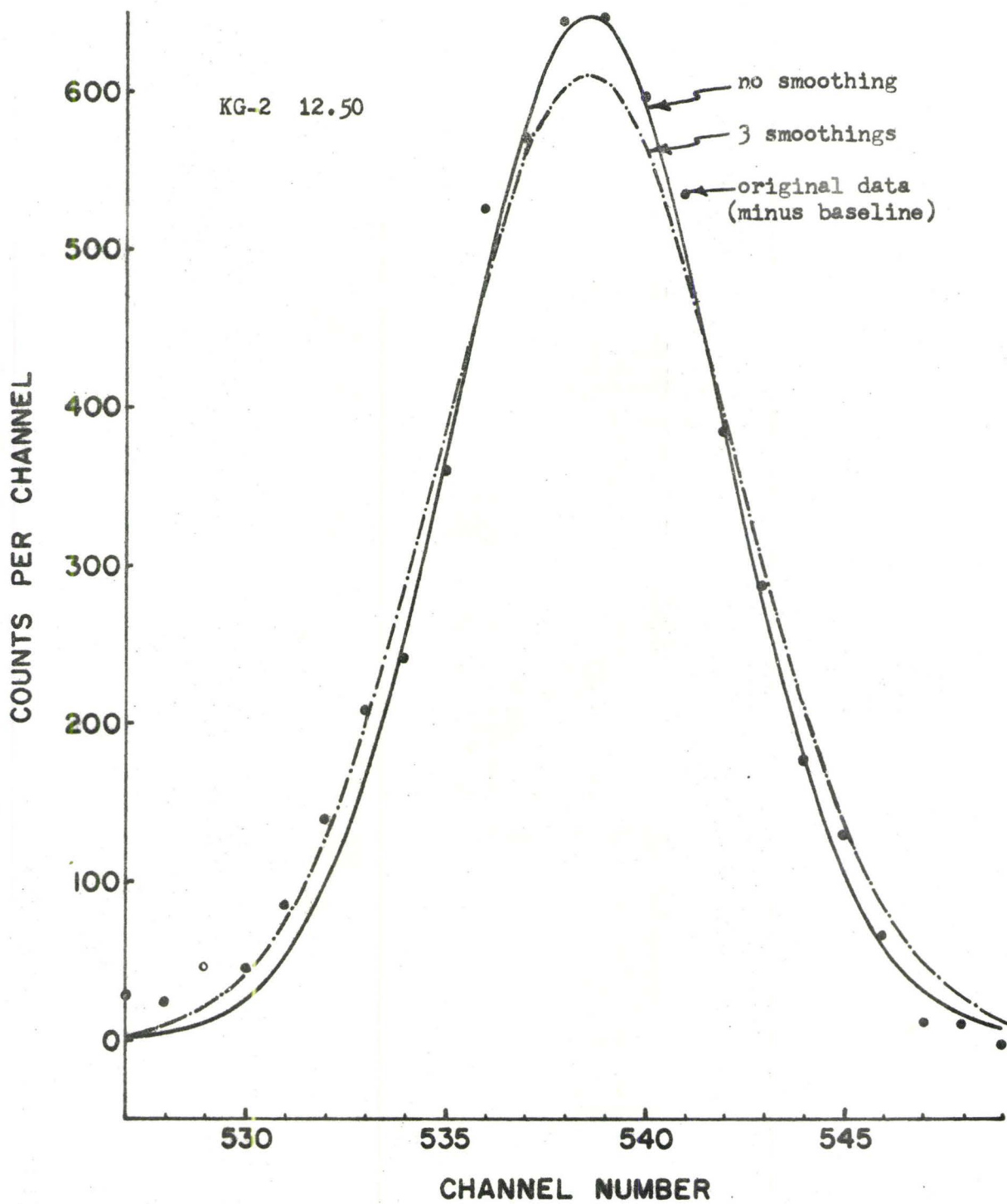


Figure 9 Effect of smoothing on the shape of the Gaussian function.

A FORTRAN IV COMPUTER PROGRAM FOR HANDLING γ - SPECTRUM DATA FROM
NEUTRON ACTIVATION ANALYSIS

```

C      STEP 1      READ IN DATA
C
      DIMENSION Y(200), Z(200), BX(200), BY(200), ZR(200), A(5)
      READ (5,1) NAME, XI, XF, Q, R, S, T, U, V
1     FORMAT (A10, 8F5.0)
      N = IFIX(XF - XI + 1.0)
      READ (5,2) (Y(I), I = 1,N)
2     FORMAT (10F7.0)

C
C      STEP 2      SEPARATE BASELINE ARRAYS, BX AND BY
C
      BX(1) = Q - XI + 1.0
      M1 = IFIX(R - Q)
      DO 3 I = 1, M1
      BX(I + 1) = BX(I) + 1.0
3     CONTINUE
      BX(M1 + 2) = S - XI + 1.0
      M2 = IFIX(T - S)
      K = M1 + 2
      L = M1 + M2 + 1
      DO 4 I = K, L
      BX(I + 1) = BX(I) + 1.0
4     CONTINUE
      BX(L + 2) = U - XI + 1.0
      M3 = IFIX(V - U)
      K2 = L + 2
      L2 = M1 + M2 + M3 + 2
      DO 5 I = K2, L2
      BX(I + 1) = BX(I) + 1.0
5     CONTINUE
      L3 = L2 + 1
      DO 6 I = 1, L3
      XJ = BX(I)
      J = IFIX(XJ)
      BY(I) = Y(J)
6     CONTINUE

C
C      STEP 3      FIT POLYNOMIAL TO BASELINE VALUES
C
      CALL POLFIT(BX, BY, BY, L3, 4, -1, A, CHISQR)

C
C      STEP 4      SUBTRACT BASELINE
C
      XB = 0.0
      DO 7 I = 1, N
      XB = XB + 1.0
      YB = A(1)+A(2)*XB+A(3)*XB*XB+A(4)*XB*XB*XB
      Z(I) = Y(I) - YB
      ZR(I) = Z(I)
7     CONTINUE

```

```

C      STEP 5      SMOOTH DATA BY AVERAGING ADJACENT CHANNELS
C
      MAX = N - 1
20 DO 9 J = 1, 3
      Y1 = ZR(1)
      DO 8 I = 1, MAX
      Y2 = (Y1+2.0*ZR(I)+ZR(I+1))/4.0
      Y1 = ZR(I)
      8 ZR(I) = Y2
      ZR(N) = (Y1+3.0*Y(N))/4.0
      9 CONTINUE

C
C      STEP 6      LOCATE TOP OF PEAK, B
C
      B = ZR(1)
      NM1 = N - 1
      DO 11 I = 1, NM1
      P = ZR(I+1) - B
      IF(P) 11, 11, 10
10 B = ZR(I+1)
      ICENT = I+1
11 CONTINUE

C
C      STEP 7      DETERMINE PEAK WIDTH (=2/H) AT B/E
C
      BE = B/2.71828
      DO 14 I = 1, 100
      K = ICENT - I
      D = BE - ZR(K)
      IF(D) 14, 13, 12
12 J1 = K
      J2 = K + 1
      GO TO 15
13 J2 = K
      J1 = J2
      GO TO 15
14 CONTINUE
15 DO 18 I = 1, 100
      K = ICENT + I
      D = BE - ZR(K)
      IF(D) 18, 17, 16
16 J4 = K
      J3 = K - 1
      GO TO 19
17 J3 = K
      J4 = J3
      GO TO 19
18 CONTINUE
19 YA = ZR(J1)
      YB = ZR(J2)
      YC = ZR(J3)
      YD = ZR(J4)
      XA = FLOAT(J1)
      XB = FLOAT(J2)

```

```

XC = FLOAT(J3)
XD = FLOAT(J4)
XE = (XB-XA)*(BE-YA)/(YB-YA) + XA
XFF = (XD-XC)*(YC-BE)/(YC-YD) + XC
CENT = (XFF + XE)/2.0
H = 2.0/(XFF - XE)

```

C
C
C
C
C
C

```
STEP 8 DETERMINE AREA UNDER CURVE
```

```
AREA = (B*1.7724539)/H
```

```
STEP 9 OUTPUT
```

```

WRITE(6,50) NAME, XI, XF
50 FORMAT(10X,8HSAMPLE ,A10,10X,9HCHANNELS ,F5.0,3X,4HTO
-,F5.0//)
WRITE(6,51) (Y(I),I = 1, N)
51 FORMAT(5X,10F7.0)
WRITE(6,54) (A(I),I = 1, 4)
54 FORMAT(/10X,12HPOLYNOMIAL ,F7.2,2H +,F7.4,4H X +,F7.4,
-7H X**2 +,F6.4,6H X**3 /)
WRITE(6,55) CHISQR
55 FORMAT(10X,14HCHI SQUARED = ,F10.5//)
WRITE(6,53)
53 FORMAT(10X,28HDATA-BASELINE , NO ROUNDING /)
WRITE(6,56) (Z(I),I = 1, N)
56 FORMAT(5X,10F7.0)
WRITE(6,59)
59 FORMAT(/10X,12HROUNDED DATA /)
WRITE(6,57) (ZR(I),I = 1, N)
57 FORMAT(5X,10F7.0)
WRITE(6,58) AREA
58 FORMAT(/10X,7HAREA = ,F10.2/)

```

C
C
C

```
OPTION 1 GAUSSIAN DISTRIBUTION
```

```

XINITL = CENT - 3.0/H
XFINAL = CENT + 3.0/H
XINC = 0.1
CALL GAUSS(B,H,CENT,XINITL,XFINAL,XINC,XI)

```

C
C
C

```
OPTION 2 PLOT DATA
```

```

X = 0.0
DO 60 I = 1, N
X = X + 1.0
CALL PLOTPT(X,Y(I),9)
60 CONTINUE
CALL OUTPLT
WRITE(6,50) NAME, XI, XF
X = 0.0
DO 61 I = 1, N
X = X + 1.0
CALL PLOTPT(X,Z(I),9)

```

```
61 CONTINUE
  CALL OUTPLT
  WRITE(6,50) NAME, XI, XF
  X = 0.0
  DO 62 I = 1, N
  X = X + 1.0
  CALL PLOTPT(X,ZR(I),9)
62 CONTINUE
  CALL OUTPLT
  WRITE(6,50) NAME, XI, XF
  STOP
  END
```

SUBROUTINE POLFIT (X,Y,SIGMAY,NPTS,NTERMS,MODE,A,CHISQR)

REF-BEVINGTON,P.R.(1969), DATA REDUCTION AND ERROR ANALYSIS
FOR THE PHYSICAL SCIENCES, MCGRAW-HILL

PURPOSE

MAKE A LEAST-SQUARES FIT TO DATA WITH A POLYNOMIAL CURVE
 $Y=A(1)+A(2)*X+A(3)*X**2+A(4)*X**3+ . . .$

DESCRIPTION OF PARAMETERS

X - ARRAY OF DATA POINTS FOR INDEPENDENT VARIABLE
Y - ARRAY OF DATA POINTS FOR DEPENDENT VARIABLE
SIGMAY - ARRAY OF STANDARD DEVIATIONS OF Y DATA POINTS
NPTS - NUMBER OF PAIRS OF DATA POINTS
NTERMS - NUMBER OF COEFFICIENTS (DEGREE OF POLYNOMIAL+ 1)
MODE - DETERMINES METHOD OF WEIGHTING LEAST-SQUARES FIT
+1 (INSTRUMENTAL) WEIGHT(I) = 1./SIGMAY(I)**2
0 (NO WEIGHTING) WEIGHT(I) = 1.
-1 (STATISTICAL) WEIGHT(I) = 1./Y(I)
A - ARRAY OF COEFFICIENTS OF POLYNOMIAL
CHISQR - REDUCED CHI SQUARE FOR FIT

COMMENTS

DIMENSION STATEMENT VALID FOR NTERMS UP TO 10

DOUBLE PRECISION SUMX, SUMY, XTERM, ARRAY, CHISQ
DIMENSION X(1), Y(1), SIGMAY(1), A(1)
DIMENSION SUMX(19), SUMY(10), ARRAY(10,10)

ACCUMULATE WEIGHTED SUMS

```

11 NMAX = 2*NTERMS - 1
   DO 13 N=1, NMAX
13 SUMX(N) = 0.
   DO 15 J= 1, NTERMS
15 SUMY(J) = 0.
   CHISQ = 0.
21 DO 50 I= 1, NPTS
   XI = X(I)
   YI = Y(I)
31 IF (MODE) 32, 37, 39
32 IF (YI) 35, 37, 33
33 WEIGHT = 1. / YI
   GO TO 41
37 WEIGHT = 1.
   GO TO 41
35 WEIGHT = 1. / (-YI)
   GO TO 41
39 WEIGHT = 1. / SIGMAY(I)**2
41 XTERM = WEIGHT
   DO 44 N= 1, NMAX
   SUMX(N) = SUMX(N) + XTERM
44 XTERM = XTERM * XI

```

```

45 YTERM = WEIGHT*YI
   DO 48 N= 1, NTERMS
   SUMY(N) = SUMY(N) + YTERM
48 YTERM = YTERM * XI
49 CHISQ = CHISQ + WEIGHT*YI**2
50 CONTINUE

```

C
C
C

CONSTRUCT MATRICES AND CALCULATE COEFFICIENTS

```

51 DO 54 J= 1, NTERMS
   DO 54 K= 1, NTERMS
   N = J + K - 1
54 ARRAY(J,K) = SUMX(N)
   DELTA = DETERM (ARRAY, NTERMS)
   IF (DELTA) 61, 57, 61
57 CHISQR = 0.
   DO 59 J= 1, NTERMS
59 A(J) = 0.
   GO TO 80
61 DO 70 L= 1, NTERMS
62 DO 66 J= 1, NTERMS
   DO 65 K= 1, NTERMS
   N = J + K - 1
65 ARRAY(J,K) = SUMX(N)
66 ARRAY(J,L) = SUMY(J)
70 A(L) = DETERM(ARRAY, NTERMS) / DELTA

```

C
C
C

CALCULATE CHI SQUARE

```

71 DO 75 J= 1, NTERMS
   CHISQ = CHISQ - 2.*A(J)*SUMY(J)
   DO 75 K= 1, NTERMS
   N = J + K - 1
75 CHISQ = CHISQ + A(J)*A(K)*SUMX(N)
76 FREE = NPTS - NTERMS
77 CHISQR = CHISQ / FREE
80 RETURN
   END

```

FUNCTION DETERM (ARRAY, NORDER)

PURPOSE

CALCULATE THE DETERMINANT OF A SQUARE MATRIX

DESCRIPTION OF PARAMETERS

ARRAY - MATRIX

NORDER - ORDER OF DETERMINANT (DEGREE OF MATRIX)

COMMENTS

THIS SUBPROGRAM DESTROYS THE INPUT MATRIX ARRAY
DIMENSION STATEMENT VALID FOR NORDER UP TO 10

DOUBLE PRECISION ARRAY, SAVE
DIMENSION ARRAY(10,10)

10 DETERM = 1.

11 DO 50 K= 1, NORDER

INTERCHANGE COLUMNS IF DIAGONAL ELEMENT IS ZERO

IF (ARRAY(K,K)) 41, 21, 41

21 DO 23 J= K, NORDER

IF (ARRAY(K,J)) 31, 23, 31

23 CONTINUE

DETERM = 0.

GO TO 60

31 DO 34 I= K, NORDER

SAVE = ARRAY(I,J)

ARRAY(I,J) = ARRAY(I,K)

34 ARRAY(I,K) = SAVE

DETERM = -DETERM

SUBTRACT ROW K FROM LOWER ROWS TO GET DIAGONAL MATRIX

41 DETERM = DETERM * ARRAY(K,K)

IF (K .- NORDER) 43, 50, 50

43 K1 = K + 1

DO 46 I= K1, NORDER

DO 46 J= K1, NORDER

46 ARRAY(I,J) = ARRAY(I,J) - ARRAY(I,K)*ARRAY(K,J)/ARRAY(K,K)

50 CONTINUE

60 RETURN

END

SUBROUTINE GAUSS(A,H,XM,XINITL,XFINAL,XINC,XI)

C
C
C
C
C
C
C
C
C
C
C

GENERATES GAUSSIAN DISTRIBUTION

$$\text{GAUSS}(X) = A \cdot \exp(-H^{**2} * (X - XM)^{**2})$$

A - MAXIMUM HEIGHT OF PEAK AT X = XM
H - 2/H = PEAK WIDTH AT A/E
XM - VALUE OF X AT CENTRE OF PEAK
XINITL - FIRST VALUE OF X
XFINAL - LAST VALUE OF X
XINC - INCREMENT OF X
XI - CHANNEL NUMBER OF FIRST Y VALUE

DIMENSION FGAUSS(5)

X = XINITL - XM

INITL = IFIX(X)

X = FLOAT(INITL)

FIRST = XI + XINITL - 1.0

WRITE(6,4) FIRST, XINC

4 FORMAT(10X,22HGAUSS(X) FROM CHANNEL ,F4.0,13H ,INCREMENT=
-,F4.2/)

XNO = (XFINAL - XINITL)/XINC

NROWS = IFIX(XNO)/10 + 1

DO 1 J= 1, NROWS

L = J + 1

XDEL2 = FLOAT(L)*XINC*5.0

DO 3 I= 1, 5

K = I - 1

XDEL1 = FLOAT(K)*XINC

FGAUSS(I) = A EXP((-H**2)*((X+XDEL1+XDEL2)**2))

3 CONTINUE

WRITE(6,2) (FGAUSS(I),I = 1,5)

2 FORMAT (10X,5F10.2)

1 CONTINUE

RETURN

END